# Gut dysbiosis promotes islet-autoimmunity by increasing T-cell attraction in islets via CXCL10 chemokine

Sakari Pöysti[†,1], Satu Silojärvi[†,1], Thomas C. Brodnicki[2], Tara Catterall[2], Xin Liu[2], Leanne Mackin[2], Andrew D. Luster[3], Thomas W.H. Kay[2], Urs Christen [4], Helen E. Thomas[2] and Arno Hänninen* [1,5]

*Running title:* Pathobiont-induced CXCL10 primes islets to T cells

[†]These authors should be considered joint first author; [1]Institute of Biomedicine, University of Turku, Turku, Finland; [2] St. Vincent's Institute of Medical Research, Melbourne, VIC, Australia; [3] Center for Immunology and Inflammatory Diseases, Division of Rheumatology, Allergy and Immunology, Massachusetts General Hospital, Harvard Medical School, Boston, MA, USA; [4] Klinikum der Goethe Universität Frankfurt, Frankfurt am Main, Germany; and [5] Turku University Hospital laboratory division, Turku, Finland.

**Corresponding author**

Arno Hänninen

MedD 7022, Kiinamyllynkatu 10, FIN-20520 Turku; Finland

Tel.: +358-50 5119870; email: arno.hanninen@utu.fi

**Footnote**

Arno Hänninen (arno.hanninen@utu.fi) and Helen Thomas (hthomas@svi.edu.au) share senior authorship.

## Abstract

CXCL10 is an IFNγ-inducible chemokine implicated in the pathogenesis of type 1 diabetes. T-cells attracted to pancreatic islets produce IFNγ, but it is unclear what attracts the first IFNγ -producing T-cells in islets. Gut dysbiosis following administration of pathobionts induced CXCL10 expression in pancreatic islets of healthy non-diabetes-prone (C57BL/6) mice and depended on TLR4-signaling, and in non-obese diabetic (NOD) mice, gut dysbiosis induced also CXCR3 chemokine receptor in IGRP-reactive islet-specific T-cells in pancreatic lymph node. In amounts typical to low-grade endotoxemia, bacterial lipopolysaccharide induced CXCL10 production in isolated islets of wild type and RAG1 or IFNG-receptor-deficient but not type-I-IFN-receptor-deficient NOD mice, dissociating lipopolysaccharide-induced CXCL10 production from T-cells and IFNγ. Although mostly myeloid-cell dependent, also β-cells showed activation of innate immune signaling pathways and Cxcl10 expression in response to lipopolysaccharide indicating their independent sensitivity to dysbiosis. Thus, CXCL10 induction in response to low levels of lipopolysaccharide may allow islet-specific T cells imprinted in pancreatic lymph node to enter in healthy islets independently of IFN-g, and thus link gut dysbiosis to early islet-autoimmunity via dysbiosis-associated low-grade endotoxemia.



## Keywords

Chemokines; IP-10 / CXCL10; CXCR3; type 1 diabetes; insulitis; beta-cell autoimmunity; IGRP-reactive T-cells; low-grade endotoxemia; type-I-interferon-signaling; *Ruminococcus gnavus*

## 1. Introduction

Type 1 diabetes (T1D) is an autoimmune-mediated disease, the incidence of which has been increasing especially in those carrying genetic variants conferring only mild or intermediate susceptibility. This suggests that in many cases, environmental factors impact strongly on T1D development. Among a multitude of candidates, factors influencing T1D development could relate to delayed or altered exposure to microbes including viruses with tropism to pancreatic islets [1, 2], to the increase in general hygiene, to changes in diet and nutrition, or to changes in gut microbiota [3, 4]. These may affect immune reactivity to environmental and self-antigens, including T1D-related autoantigens. Gut microbiota alterations in T1D and islet-autoimmunity have been widely studied [5], and gut dysbiosis proposedly predisposes to T1D [6] as well as other autoimmune diseases [7]. Recent prospective studies of the gut microbiota metagenome in children at risk of developing T1D suggest that a scarcity of microbes capable of producing short-chain fatty acids (SCFA) associates with progression of islet-autoimmunity [8, 9]. Scarcity of SCFA may deter epithelial integrity essential to its function as a barrier to microbial contacts with the host, but it is unclear how this could promote autoimmunity to beta cells in pancreatic islets.

Autoimmunity to beta cells initiates in pancreatic lymph nodes by activation of islet-reactive T cells differentiating into IFNγ producing Th1 helper T cells and cytotoxic CD8 T cells. After their egress from pancreatic lymph nodes and recirculation in blood, they home to pancreatic islets by chemotaxis. This involves receptor-ligand interactions between chemokine receptors on T cells and corresponding chemokine ligands expressed in the islets. Th1 and cytotoxic T cells typically express the CXCR3 chemokine receptor that binds to CXCL9, CXCL10 and CXCL11 chemokines [10]. Among other chemokines, levels of CXCL9 and CXCL10 are elevated in sera of children with T1D and in adults with recent-onset T1D [11-13]. Pancreatic islets and especially islet beta cells express high levels of CXCL10 in individuals with recent onset T1D [14-16] and in animal models [15, 17-20]. Cytokines can also induce cultured islets to produce CXCL10, along with CXCL9 and CCL8 [15].

Despite identification of the IFNγ–inducible CXCL10 as potentially one of the most important chemokines in T1D, the stimuli that direct the entry of the "first" diabetogenic T cells into healthy islets prior to the existence of IFNγ–producing cells in islets remain elusive. Although tissue-resident memory T cells exist in many tissues [21], there is little evidence for T cells residing in healthy islets, albeit preproinsulin-specific T cells have been identified in pancreatic exocrine tissue of healthy individuals [22]. NK cells also exist in the pancreas of non-diabetes prone mouse strains, and some of these may produce IFNγ during early stages of islet-autoimmunity [23]. Islets also contain dendritic cells and macrophages fulfilling homeostatic roles in islet development, but despite some evidence of IFNγ production by macrophages [24, 25], they are more likely to produce cytokines other than IFNγ upon stimulation. Islet-macrophages and beta cells themselves express toll-like receptors (TLRs) and other pattern recognition receptors [26] making them responsive to microbes and microbial structures such as viruses in the close environment. Due to rich capillary networks surrounding islets, macrophages and possibly beta cells themselves can also react to microbial stimuli in the blood circulation. Therefore, an increase in the levels of microbial stimuli even only in the circulation may exceed or lower the threshold needed for triggering the production of proinflammatory cytokines and chemokines within the pancreatic islets [27].

Conditions in which host-microbe symbiosis is disturbed may lead to impaired gut barrier function and endotoxin leakage from the gut [28]. Using *R. gnavus* [29] and *C. rodentium* [30] as intestinal pathobionts to model gut dysbiosis, we investigated if dysbiosis or lipopolysaccharide affects islet chemokine- and TLR-expression *in vivo*, and evaluated endotoxin as a potential inducer of CXCL10 induction in healthy islets *in vitro*. Our results indicate that pathobiont-induced dysbiosis promotes CXCL10 expression in islets and that this requires TLR-4 signaling. In the absence of IFNγ, CXCL10 production is induced by lipopolysaccharide in islets via type I IFN signaling -and relies mostly on islet macrophages. At the transcriptome level, also islet beta cells display LPS-induced *Cxcxl10* expression together with activation of type-I-interferon, TNF- and TLR-4 signaling pathways. These combined results suggest that gut dysbiosis makes islets accessible to autoimmune T cells at the earliest phases

of T1D pathogenesis and that this involves LPS, which may explain the innate interferon response reported also previously in islets of NOD mice [17].

## 2. Materials and methods

### 2.1. Mice

NOD/ShiLtJ, 8.3-NOD (NOD.Cg-Tg(TcraTcrbNY8.3)1Pesa/DvsJ) and TLR4-KO (B6(Cg)-Tlr4tm1.2Karp/J) mice were purchased from Jackson Laboratory and maintained in University OF…. Rag1-KO (NOD.Cg-Rag1$^{tm1/Mom}$/J) were purchased from Jackson Laboratory and were maintained at … Institute. CRISPR/Cas9 gene editing was performed by the… Phenomics … to target *Ifnar1*, *IFNγr1 and ifnlr* in the NOD mouse strain. Briefly, single-guide RNAs (sgRNA) were designed to generate premature stop-codon mutations within *Ifnar1* (sgRNA 5'GCTCGCTGTCGTGGGCGCGG3'), *IFNγr1* (sgRNA 5'CTGTCTGCGAAGGTCGGGAG3') or *Ifnlr1* (sgRNA 5'GAGTAGGGGCGCCCACCGGT3'). The sgRNA and Cas9 mRNA were co-injected into NOD/ShiLtJArc embryos, which were used to generate $G_0$ offspring. Selective backcross and intercross breeding were subsequently performed to establish mutant NOD lines that are deficient for the different interferon receptors - IFN-$\alpha$ receptor (IFNAR), IFN-$\gamma$ receptor (IFNGR) or IFN-$\lambda$ receptor (IFNLR): NOD.*Ifnar1*$^{em16/em16}$ (em16: 5 base pair deletion at chr16:91,485,359 = 30 amino acids + stop codon), NOD.*IFNγr1*$^{em15/em15}$ (em15: 7 base pair deletion at chr10:19,592,149 = 24 amino acids + stop codon), and a triple mutant line NOD.*Ifnar1*$^{em16/em16}$*IFNγr1*$^{em15/em15}$*Ifnlr1*$^{em13/em13}$ (em13: 16 base pair deletion at chr4:135,686,546 = 13 amino acids + stop codon).

The animals were maintained in individually 322 ventilated cages (IVC) under controlled conditions with temperature 21 ± 3ºC, relative humidity 55 ± 15 % 323 and 12 h light and 12 h dark light cycle. The mice were fed *ad libitum* with CRM (E) diet (Special Diet Services, 324 Witham, Essex, England) and water was provided *ad libitum.*

**2.2. Induction of dysbiosis in mice**

We modelled dysbiosis by inoculating mice with either of two microbes, a murine pathogen or a human pathobiont. *Citrobacter rodentium* (*C. rodentium*) is an intestinal mouse pathogen used to induce colitis, which in healthy mice is self-limiting [31] and in our mouse colonies, induces mainly local inflammatory changes in the intestine with an alteration in overall microbiota composition (manuscript submitted) and subclinical or mild clinical disease [32]. *Ruminococcus gnavus* (*R. gnavus)* is commonly present in microbiota of even healthy humans, but competes with other members of healthy microbiota and is considered a pathobiont, because its ample representation associates with inflammatory pathologies of the gut [29].

To induce dysbiosis with *Citrobacter rodentium, C. rodentium* (strain ICC168) was cultured overnight in liquid broth in the presence of nalidixic acid (50mg/L). After centrifugation of the culture, bacteria were resuspended in a volume allowing 1 x $10^9$ bacteria to be administered in a 200 µl volume by oral gavage. Control (CTRL) mice received same volume of culture medium.

To induce dysbiosis with *R. gnavus*, mice were first treated with a cocktail of broad-spectrum antibiotics (ampicillin 100mg/kg, vancomycin 50mg/kg, neomycin 100mg/kg and metronidazole 100mg/kg) by oral gavage five (5) days prior to infection with *R. gnavus*. *R. gnavus* (a clinical isolate obtained from Turku University Hospital laboratory and identified by MALDI-TOF) was cultured in fastidious anaerobe (FAB) broth (+ 5g/L glucose) in strictly anaerobic conditions at 37 °C for 48 hrs. After centrifugation of the culture, bacteria were resuspended in PBS in a volume of 200 µl (1 x $10^7$ bacteria) and administered by oral gavage as described above. Control mice were administered PBS at the same volume. Our initial experiments detected individual variation in the effects of *R. gnavus* inoculation on gut cytokine profiles and gut permeability measures, and therefore, colon RNA from each mouse was analysed with RT-qPCR (Figure S1). Three quarters (75%) of mice showed clearly elevated expression of *Il1b* and *Reg3γ*, and were included in further analyses.

### 2.3. Evaluation of diabetes development and islet inflammation

To analyse if dysbiosis affects diabetes development, 4 weeks old NOD mice were treated with *C. rodentium* or medium and were monitored for onset of diabetes until 20 weeks of age. The blood glucose concentration was measured (Contour, Bayer, Germany) weekly after 12 weeks of age by tail vein puncture. Mice having a blood glucose concentration greater than 12mM for two consecutive days were diagnosed as diabetic.

Insulitis was quantified 2 weeks after treatment with either *C. rodentium,* or *R. gnavus* and the cocktail of antibiotics by scoring individual islets for mononuclear cell infiltration using cryopreserved pancreas sections (5µm) stained with H&E. At least 60 individual islets per pancreas were each scored as follows: 0, no insulitis; 1, peri-insulitis with or without minimal infiltration in islets; 2, insulitis with <50% infiltration of islets; 3, invasive insulitis with >50% infiltration of islets.

### 2.4. Induction of CXCL10 in islets by *in vivo* LPS treatment

To determine if elevated LPS levels *in vivo* induce CXCL10 expression in islets similarly to dysbiosis and if this requires IFN-signaling, LPS from E. coli (Sigma-Aldrich) was injected in a dose of 30 µg into the peritoneal cavity of wild-type and genetically modified NOD mice (described above) and to wild-type and Tlr4-KO C57/Bl mice (described above). After 48 hours, pancreases were snap frozen in liquid nitrogen into Eppendorf tubes. Samples were shipped to Finland on dry ice and processed for immunohistochemistry as described below.

### 2.5. Immunohistochemistry of pancreatic islets

Pancreases were snap frozen in Eppendorf tubes immersed in liquid nitrogen and embedded in Tissue-Tek OCT before sectioning. 6 µm frozen sections were placed on Superfrost plus slides (Thermo Scientific, Waltham, MA, USA) and fixed with cold acetone at -20°C for 5 min. The sections were stained using the Shandon Sequenza Immunostaining slide rack with Shandon coverplates (Thermo Scientific, Waltham, MA, USA). The sections were blocked with 3% BSA and stained with primary Ab for 50 min at RT and secondary Ab for 30 min at RT. The antibodies and concentrations used are listed in Table S2. The stained sections were mounted with ProLong Diamond Antifade Mountant (Molecular Probes, USA) and visualized with Nikon Eclipse Ti-2 microscope (Japan) and photographed with Hamamatsu Orca C13440 Flash4.0 ERG (b/w) ccd camera (Japan). CXCL10-expression was analyzed in a minimum of 20 islets sampled from different levels of each pancreas and quantified as fluorescence intensity using ImageJ software. Results are presented as arbitrary units of mean fluorescence intensities (MFI) as calculated based on the sampled islets.

### 2.6. CXCL10 production *ex vivo* from stimulated islets

Islets were isolated from 6-8-week-old male NOD mice using collagenase P (Roche, Basel, Switzerland) and Histopaque-1077 (Sigma-Aldrich, USA) density gradient centrifugation as previously described [33]. Islets were handpicked and cultured at 50 islets/well in 200 µl complete CMRL medium containing 10% FCS, 100 U/ml penicillin, 100 mg/ml streptomycin and 2 mM L-glutamine, in a 37°C, 5% $CO_2$ humidified incubator. IFNγ (Biolegend) was added at 100 U/ml and LPS (LPS-EB Ultrapure, Jomar Life Research) was added at 10, 50 or 250 ng/ml. Islets were cultured for 2 or 4 days then subjected to 6 freeze/thaw cycles, centrifuged and 100 µl of the undiluted supernatant was used assayed for mouse CXCL10 by ELISA (R&D Systems, USA). CXCL10 concentrations were calculated from a standard curve using GraphPad Prism version 9.

### 2.7. *In vivo* TLR4 inhibition

To determine if blocking TLR4 signalling affects CXCL10 induction during dysbiosis, 5-week-old NOD mice were injected daily (i.p.) with TAK-242 (3mg/kg in PBS; Calbiochem, San Diego, USA). Dysbiosis was induced in NOD mice with *C. rodentium* (described above), and pancreatic islets were analysed for CXCL10 expression by immunohistochemistry (described above).

### 2.8. CXCL10 antibody treatment

The function-blocking CXCL10 antibody 1F11 was produced as previously described [34, 35] and used to block CXCL10 *in vivo*. NOD mice were treated 3 times per week by intraperitoneal injection of 100 µg of 1F11 or isotype control (*InVivo*MAb Armenian hamster IgG, Bio X Cell, USA) from the age of 4 weeks to 8 weeks. After the treatment, pancreases were collected for insulitis analysis (described above).

### 2.9. Flow Cytometry

For flow cytometry lymph node (LN) samples were collected in RPMI media. Single cell suspensions were made by digesting lymph nodes with collagenase (100µg/ml, 10min, 37°C, Sigma-Aldrich, USA) and pressing cells through metal mesh. Cells were filtered through nylon membrane (77µm), stained with trypan blue stain (1:1, Biorad), and counted using a TC-20 automated cell counter (Biorad, USA). Staining of the cell-surface markers was performed using selected antibodies in stain buffer (PBS, 2% FCS, 0.01% NaN3) for 15 min at 4°C. Zombie dye was used to exclude dead cells. T cells were identified by staining with Brilliant Violet 785 conjugated anti-CD45 (clone: 30-F11, BioLegend), Brilliant Violet

510 conjugated anti-TCRβ (clone: H57-597, BioLegend), FITC conjugated anti-CD4 (clone: GK1.5, BioLegend) and APC-Cy7 conjugated anti-CD8 (clone: 53-6.7, BioLegend) antibodies. To analyze T-cell activation in 8.3 NOD mice, cells were stained with PerCP-Cy5.5 conjugated anti-CD44 (clone: IM7, BioLegend) and PE conjugated anti-CD69 (clone: H1.2F3, BioLegend). Insulin B15-23 (VYLKTNVFL) and IGRP 206-214 (LYLVCGERG) in complex with H2K(d) MHC tetramers conjugated to allophycocyanin (APC) and phycoerythrin (PE)-conjugated LO91-99 tetramer as an irrelevant control peptide were obtained from NIH Tetramer Core Facility (Emory University; Atlanta, GA) and used to identify islet-specific T cells. Tetramers were diluted to 1:500 final concentration before adding to cells that were then incubated for 30 min at 4°C. CXCR3 expression on T cells was detected by staining with Brilliant Violet 421 conjugated anti-CXCR3 antibody (clone: CXCR3-173, BioLegend). Stained cells were analyzed using a NovoCyte flow cytometry (Agilent, USA) and data were analyzed with NovoExpress software (Agilent, USA).

### 2.10. Evaluation of intestinal permeability by LPS-binding protein and haptoglobin levels in serum

Intestinal permeability was analyzed by measuring LPS binding protein (LBP) and Haptoglobin from serum. Blood was collected into coagulation activator containing tubes and serum was prepared by centrifugation. The sera were frozen at -20°C until analysis. Mouse LBP ELISA Kit (ABCAM, ab213876, Cambridge, UK) was used to measure LBP and mouse Haptoglobin ELISA Kit (ABCAM, ab272472, Cambridge, UK) was used to measure Haptoglobin according to manufacturer's instructions and using 1:10 000 and 1:100 dilutions.

### 2.11. Depletion of macrophages in islet cultures

To deplete macrophages freshly isolated islets of 6-9 week old male NOD mice were incubated at 50 islet/well in a 96-well plate with 0.25 mg/ml clodronate liposomes (Liposoma BV, Amsterdam, Netherlands) resulting typically in more than 80% depletion of F4/80+ cells (Suppl. Figure 4). LPS (LPS-EB Ultrapure, Jomar Life Research) was added at 10ng/ml and IFNγ (Biolegend) at 100 U/ml where indicated. Islets were cultured for 2 days before collecting supernatant which was assayed for mouse CXCL10 by ELISA (R&D Systems, USA) as described above.

### 2.12. RNA-seq analysis

Islets isolated from 6–9-week-old male NOD mice were hand-picked into 1 ml dishes and cultured for 48 h with 10 ng/ml LPS or left untreated. Islets were then treated with trypsin to prepare single-cell suspensions, which were stained with anti-CD45 to sort endocrine cells apart from leukocytes. Beta cells were further sorted apart of non-beta cells on the basis of their autofluorescence. The experiment was repeated on 3 independent days with total of n=5 independent replicates.

Paired-end RNA-seq libraries were constructed using the Illumina TruSeq mRNA Library Prep Kit and sequenced on an Illumina NovaSeq 6000 at the Australian Genome Research Facility. 150bp paired-end reads were subjected to quality control by FastQC (version 0.11.9). Low quality reads were trimmed with Trimmomatic (version 0.40) using a sliding window trimming method, which scans from 5’ end of a read and clips the read once below the average quality score of Q28 within the 4bp window size. Any reads with Nextera Transposase sequences had to be trimmed off. STAR genome index was built based on Ensembl mouse genome (Mus_musculus.GRCm39). The processed reads were aligned by STAR (version 2.6.1a) and quantified by HTSeq-count (version 2.0.2). DESeq2 (version 1.36.0) was used to determine gene expression changes and differentially expressed genes were extracted to perform gene ontology and pathway enrichment analysis by gprofiler2 (version 0.2.1).

### 2.13. Real-time PCR analysis

Islets were isolated from individual Rag-/- NOD mice and stimulated with LPS for 48 hours. Beta cells were sorted as described above and, total RNA was isolated from approximately 5,500 to 15,500 (average 10,200) beta cells per mouse using the ISOLATE RNA Micro kit (Bioline). First strand cDNA was generated using PrimeScript RT reagent Kit (Takara) according to the manufacturer's instructions. cDNA was diluted 1:5 and real-time PCR analysis was performed on a LightCycler 480 (Roche) using Perfecta QPCR Fastmix II (Quanta Biosciences). Taqman gene expression primers for murine Cxcl10 (Mm00445235) and Actb (Mm00607939_s1) were used (Applied Biosystems). Ct values were normalized to the Ct values of actin and expressed as dCt.

### 2.14. Statistical analysis

Statistical significance for comparisons between two groups was calculated by unpaired two-tailed Student's t-test. For comparisons between multiple groups, p-values were calculated by one-way ANOVA followed by Dunnett's or Tukey's multiple comparison where indicated. Differences between expression levels of transcripts were expressed as -log10 adjusted p value.

### 2.15. Ethics approval

Experimentation on animals was approved by national authorities either in Finland (National Animal Experiment Board of Finland (License number: ESAVI/19866/2019; ESAVI/479/04.10.07/2016) in accordance with the EU Directive 2010/63/EU) or in Australia (St Vincent's Hospital Animal Ethics Committee number 017/17; 013/20).

# 3. Results

### 3.1. Gut dysbiosis induces CXCL10 expression in islets and accelerates islet-autoimmunity

To verify results from a number of earlier studies (reviewed in [36], we stained pancreatic sections of 6-7 week old female NOD mice for several chemokines (CCL2, CCL4, CCL5, CXCL10 and CXCL12). Notably, CXCL10 was stained clearly in pancreatic islets, while staining for the other chemokines indicated much weaker expression (Table S1). To model dysbiosis in non-obese diabetic (NOD) mice and address the potential influence of dysbiosis on CXCL10 expression, we employed two different gut microbes, *C. rodentium* and *R. gnavus,* an enteric pathogen in mice [37] and a human pathobiont [29]. When administered to female NOD mice (once at 4 or twice at 4 and 6 weeks age; see Methods), there was no gross effect on general health or well-being, but there was increased serum concentrations of haptoglobin and lipopolysaccharide binding protein (LBP, Figure 1A, B). This is consistent with increased gut permeability resulting in gut bacteria or their components leaking into the circulation. Induction of dysbiosis by either of these bacteria was associated with increased CXCL10 expression in the pancreatic islets (Figure 1C, D). In addition, *C. rodentium*-induced dysbiosis was associated with accelerated development of insulitis during the 4-week follow-up (Figure 1E, F) and earlier onset of diabetes compared to controls (Figure 1G).

### 3.2. Lipopolysaccharide induces CXCL10 expression in islets both *in vivo* and *in vitro*

CXCL10 is produced by mouse islet cells and by NIT-1 cells in response to a combination of cytokines including IFNγ [19]. Following the finding that bacteria-induced dysbiosis and increased intestinal permeability is associated with increased CXCL10 expression in NOD islets, we investigated if mimicking the gut dysbiosis with LPS, either systemically administered or added in cultured islets of young (6-8 weeks old) NOD mice induces CXCL10 in islets. Under *in vivo* conditions, LPS injected into peritoneal cavity as a single bolus of 30 μg increased the expression of CXCL10 in the islets within 24

h, which was further accentuated after another 24 hours (Figure 2A). Compared to age-matched C57BL/6 mice, CXCL10 induction was more robust in NOD mice (Figure 2B). The propensity for enhanced CXCL10 expression in the islets following systemic administration of LPS may derive from an initial phase of ongoing immune pathology in the islets of NOD mice [38], or some basal level of general dysbiosis present in NOD mice, both of which are not evident in C57BL/6 mice. To address this further, we tested if LPS induces or augments CXCL10 production in islets *in vitro*.

Under *in vitro* conditions,–LPS increased CXCL10 secretion up to 10-fold in cultured NOD islets depending on LPS concentration (Figure 2C). As IFNγ is a potent inducer of CXCL10, we also tested the potential synergistic effect of LPS and IFNγ on CXCL10 induction. Using a concentration of IFNγ (100 U/ml), which alone induced only marginal CXCL10 production, LPS potentiated CXCL10 production 10 to 20-fold starting from as low as 10 ng/ml LPS (Figure 2C). Additional independent experiments showed that CXCL10 production was significantly increased even at the lowest concentration of LPS alone (Figure 2D). Notably, this concentration of LPS is only slightly higher than levels previously reported in the serum of mice exposed to a high-fat diet [28]. These combined observations strongly suggested that LPS not only augments induction of CXCL10 production by IFNγ, which may be relevant when IFNγ levels alone are not sufficient to induce production of CXCL10, but also that LPS can alone induce CXCL10 in concentrations relevant of low-grade inflammation (Figure 2C).

### 3.3. CXCL10 induction in islets is mediated by TLR4

LPS induces TLR4 expression in pancreatic islets *in vitro* [26] and *in vivo* (Figure S2). We therefore determined if the increased CXCL10 expression following bacteria-induced gut dysbiosis involves recognition of bacterial cell-wall components of gram-negative bacteria. We pretreated mice with the TLR4-blocking agent TAK-242 prior to *C. rodentium* administration. Compared to the levels of CXCL10 in NOD mice not receiving TAK-242 pretreatment, mice pretreated with TAK-242 expressed

significantly lower levels of CXCL10 in the islets following dysbiosis induction (Figure 3A). To confirm that induction of CXCL10 in islets is mediated through TLR4 signaling, we treated TLR4-KO mice with *C. rodentium*. While *C. rodentium* induced CXCL10 in islets of wild type C57BL/6 mice, a similar induction was not detected in TLR4-deficient C57BL/6 mice (TLR4-KO Figure 3B). Direct intraperitoneal injection of LPS also did not induce CXCL10 in the islets of TLR4-deficient C57BL/6 mice (Figure 3C).

### 3.4. Dysbiosis promotes activation of IGRP-reactive T cells expressing CXCR3 in pancreatic lymph nodes

Autoimmunity against islets initiates in the pancreatic lymph node (PLN) by activation of islet-specific T cells. Using MHC-peptide tetramers targeting T cells recognizing insulin B15-23 or islet-specific glucose-6-phosphatase catalytic subunit-related protein (IGRP) 206-214 in complex with H2K(d), we determined the effect of dysbiosis on *in vivo* activation of intrinsic T cells recognizing these autoantigens. On average, insulin-specific CD8 T cells comprised 0.5% of all CD8 T cells in the PLN of wild-type NOD mice, and induction of dysbiosis with *C. rodentium* 6 days before analysis did not increase their prevalence in PLN (Figure 4A and Figure S3). This is consistent with a previous report on the effects of co-housing on autoimmunity in NOD mice [39]. However, IGRP-specific T cells in the PLN demonstrated a significant increase with some mice having a >2-fold increase, albeit the prevalence of IGRP-specific T cells was noticeably variable between mice at 6 days post-infection with *C. rodentium* (Figure 4B and Figure S3). While only a small proportion of all CD8 T cells in PLN expressed CXCR3, a substantial proportion (up to 50%) of IGRP-specific T cells expressed CXCR3 (Figure 4C, D).

Imprinting of T cells with chemokine receptors follows the encounter with their cognate antigen presented to them in the lymph node [40]. To evaluate the imprinting efficiency of islet-specific T cells in PLN, we determined the dynamics of CXCR3 expression among transgenic, IGRP-specific 8.3 T cells based on their CD44 and CD69 expression profiles. Similar to wild-type NOD mice, dysbiosis also

affected IGRP-specific T cells in 8.3 transgenic mice, in which over 90% of CD8 cells were IGRP-specific (not shown), and this was evidenced by an increase in their CD44 expression profile (Figure 4E, F). Compared to a low level of CXCR3 expression in naive (CD44-/CD69-) cells, CXCR3 expression increased moderately during transition to the next activation phase. Consistently with the function of CD69 in mediating a signal for retention in lymph nodes, cells in the final activation state (CD44+/CD69- cells) were imprinted with CXCR3 at the highest frequency (Figure 4G). In comparison to a non-draining lymph node, this activated/memory subset (CD44+/CD69- cells) of IGRP-specific T cells was significantly more often imprinted with CXCR3 expression in PLN (Figure 4H).

### 3.5. CXCL10 mediates T-cell entry into islets during early insulitis

CXCL10 attracts especially Th1 cells and cytotoxic CD8 T cells, both implicated in islet-destructive insulitis [10]. To neutralize CXCL10 chemokine function *in vivo* we used anti-CXCL10 monoclonal antibody 1F11, which binds to free CXCL10 but not to CXCL10 attached to endothelial or other surfaces [34]. This antibody prolongs diabetes reversal in NOD mice treated with anti-CD3 antibody and delays the onset of diabetes in RIP-LCMV mice [36]. Dysbiosis was induced to 4-week-old NOD female mice with *C. rodentium*, which were treated with intraperitoneal injections of 1F11 three times a week until 8 weeks of age, after which we determined the overall level of insulitis and its cellular composition. In mice treated with 1F11, fewer lymphocytes had accumulated in islets compared to mice treated with the species- and isotype-matched antibody. Their mean insulitis score was 40% lower, and the proportion of islets determined intact (insulitis score 0) was 20% higher in 1F11–treated mice compared to control-treated mice (Figure 5A, B).

We also evaluated if blocking CXCL10 affects the accumulation of CD4 and CD8 T cells in islets as Th1 cells and cytotoxic CD8 T cells express CXCR3 and become imprinted with CXCR3 during their activation in the pancreatic lymph node, as confirmed above for IGRP-reactive CD8 T cells. Simultaneous staining

of CD4- and CD8-expressing T cells and of CD19-expressing B cells in pancreatic sections revealed a significant reduction of CD4 and CD8 T cells in relation to B cells (CD19+ cells) in islets (Figure 5C-E).

### 3.6. T cells and interferon-γ are dispensable for LPS-induced CXCL10 production in islets

Inflammatory Th1 and Tc1 cells are potent producers of IFNγ, and the prominent CXCL10 expression seen in islets of new-onset T1D and in animal models [36] likely reflects the effects of infiltrating T cells on CXCL10. To address if T cells and IFNγ are an absolute requirement for CXCL10 production in islets, we tested CXCL10 production in islets either devoid of T cells or non-responsive to IFNγ. LPS induced CXCL10 secretion in islets from RAG1-deficient NOD mice at a concentration as low as in wild-type islets. At higher LPS-concentrations, CXCL10 secretion increased comparably to wild-type islets (Figure 6A). Similarly, LPS was able to induce CXCL10 secretion in islets isolated from IFNGR-KO NOD mice. As expected, IFN-γ did not stimulate or augment LPS-stimulated CXCL10 secretion in these islets (Figure 6B).

### 3.7. Type I interferons mediate IFNγ-independent induction of CXCL10 by LPS in islets

Among other proinflammatory mediators, type I interferons induce *Cxcl10* transcripts in EndoC-βH1 beta cells [41]. The CXCL10 promoter contains a functional interferon-sensitive response element (ISRE) [42], and in murine macrophages, induction of *Cxcl10* by LPS involves IFNβ activity [43]. Accordingly, we injected LPS into the peritoneal cavity of IFNAR-KO and IFNGR-KO NOD mice, as well as NOD mice deficient for three interferon receptors: IFNAR, IFNGR and the interferonλ -receptor (IFNLR). Although CXCL10 expression increased in response to LPS in islets of both IFNAR-KO and IFNGR-KO mice, mice deficient for both IFNAR and IFNGR, as well as IFNLR ("Triple KO mice"), showed little if any response to LPS. This was consistent with both type I and type II interferon–induced

mechanisms being activated by LPS *in vivo* (Figure 6C). Thus, IFNAR and IFNGR are mutually redundant and can substitute for each other for CXCL10 induction *in vivo*. These may involve systemic effects on, for example, NK cells making IFNγ in response to LPS [44]. In cultured islets, unlike islets from IFNGR-KO mice, islets from IFNAR-KO mice showed relatively little to no CXCL10 production in response to LPS, indicating that induction of CXCL10-production in islets in response to LPS requires type I interferon signaling. In the presence of the small amount of IFNγ, IFNAR-KO NOD islets responded to LPS similarly to wild-type NOD islets suggesting synergy between LPS and type II interferon to induce CXCL10 production in islets (Figure 6D).

### 3.8. Induction of CXCL10 by LPS involves islet macrophages

During the development of islet-autoimmunity, islets become progressively infiltrated by a variety of lymphoid and myeloid cells, along with a subtype of macrophages expressing inflammatory markers and *Cxcl10* [38]. These cells may represent resident macrophages activated in the islets following the accumulation of inflammatory cells [27, 45]. However, resident macrophages may also respond to innate immune stimuli, including LPS, in islets under steady state conditions [27]. The CXCL10 promoter contains a functional nuclear factor kappa B (NF-κB) element [46], which may allow induced expression of CXCL10 by proinflammatory cytokines, such as TNF, produced by resident macrophages. Intriguingly, depletion of resident macrophages by clodronate abolished CXCL10 induction in cultured islets by LPS (Figure 6E), suggesting that CXCL10 induction by LPS requires resident macrophages. While islets devoid of macrophages made very little CXCL0 in response to LPS or TNF (Figure 6E), IFNγ in combination with LPS was able to induce a low yet appreciable level of CXCL10 production in wild-type but not IFNGR-KO islets (Figure 6E). This is consistent with islet endocrine cells producing CXCL10, which may accelerate immune cell infiltration into the islets once IFNγ is already available in the islets.

### 3.9. LPS activates broad cytokine and interferon signaling in islet beta cells

CXCL10 is made in NIT cells in response to cytokines [19], but it remains unclear if primary beta cells produce CXCL10 and in response to LPS. RNA sequence analysis of beta cells purified from dispersed islets of NOD mice following their stimulation with LPS showed immune activity on a broad scale (Figure 7). A total of 657 genes (> 2-fold increase) were differentially expressed in LPS-treated beta cells, whereas 256 genes were differentially expressed in β-cells cultured without LPS (Figure 7A). The genes upregulated by LPS included those related to molecular pathways for cytokine signaling, TNF signaling and interferon signaling, as well as MHC class I antigen processing/presentation and TLR4-activated signaling (Figure 7A, B). As would be expected based on the results described above, *Cxcl10* expression was increased in response to LPS (Figure 7A, C, D). Moreover, expression of both type I and type II interferon-receptors was upregulated in LPS-stimulated beta cells along with differential expression of genes within the TNF-signaling pathway (Figure 7B, C).

## 4. Discussion

The association of CXCL10 expression with the development of insulitis is widely documented in T1D [36]. In distressed islets of the diabetic pancreas, CXCL10 expression is detectable at relatively high levels [14], while little if any CXCL10 is detectable in islets of healthy individuals [14, 36]. Similarly, CXCL10 expression is barely detectable in young NOD mice with healthy islets, but increases as insulitis progresses during the pre-diabetic stage [15]. In the spontaneously diabetic BB rat model, CXCL10 expression in the islets also develops along with the development of islet autoimmunity. Of note, reprogramming gut microbiota development by weaning to casein hydrolysate diet reduced CXCL10 expression in diabetes-prone rats [20].

In this study, we report that gut dysbiosis accelerates insulitis and diabetes development in NOD mice, and identified CXCL10 induction in islets as the mechanism mediating this effect. We show that CXCL10 induction is dependent on TLR-4 signaling and that it associates with elevated serum levels of lipopolysaccharide-binding protein (LBP) and haptoglobin, which reflect absorption of LPS and other microbe-derived molecules and increased gut permeability. We also found it possible to inhibit dysbiosis-accelerated insulitis by neutralizing CXCL10 in mice. We show that LPS induces CXCL10 production in healthy islets in a manner in which IFNγ-signaling is redundant to type I interferon signaling. In light of our observation that LPS induces CXCL10, it is noteworthy that TLR4-/- NOD mice show accelerated diabetes incidence [47, 48]. However, TLR4 deficiency in NOD mice associated with dysregulated metabolism in the form of insulin resistance, abnormalities of energy metabolism and reduction of circulating short-chain fatty acids, all of which impact on blood glucose levels [48]. TLR4-signaling also regulates microbiota composition [49] and B-cell activation [50], thus indicating broader function for TLR4 in diabetes development than merely the induction of proinflammatory cytokines and CXCL10 expression. Pathobionts such as *C.rodentium* and *R. gnavus* may impact on diabetes development not only by increasing absorption of bacterial lipopolysaccharides from the intestine but also by metabolites produced by these and other bacteria.

Gut dysbiosis relates to a state of dysregulation in overall microbial composition or in colonization of the intestine with microbes determined as symbionts or pathobionts. Dysbiosis relates also to harmful changes in gut physiology including an increase in inflammatory activity. We modeled gut dysbiosis in mice using *R. gnavus*, which is a normal constituent of human microbiota but considered a pathobiont [29] and with *C. rodentium. C. rodentium* is considered a mouse pathogen [30], but in our colonies of wild-type mice, it induces an asymptomatic or very mild infection [32], and simultaneously, it alters microbiota composition [37]. *C. rodentium*–infection accelerates insulitis in NOD mice [51], and we found that *C. rodentium* as well as *R. gnavus* accelerated insulitis and promoted CXCL10 expression in islets of young NOD mice. Intriguingly, increased zonulin levels caused by impaired gut barrier function have been reported in individuals who later developed T1D [52, 53]. Despite such

observations, there are few insights into the underlying mechanisms associated with T1D autoimmunity. In experimental systems, evidence exists to link impaired barrier function to autoimmunity in pancreatic islets. Accordingly, experimental disturbances impairing intestinal barrier function increased activation of islet-antigen specific T cells in pancreatic lymph nodes in the BDC2.5 mouse model, as well as CD4 and CD8 T cells in the low-dose streptozotocin model [54, 55].

We used antigen-MHC tetramers to track naturally occurring insulin- and IGRP-reactive T cells in NOD mice to study the effects of pathogen-associated dysbiosis in the activation of autoreactive T cells in pancreatic lymph nodes in wild-type mice. By dissecting stages of T-cell activation in pancreatic lymph nodes, we confirm an increase in CXCR3 expression in IGRP-reactive T cells, and identify this to take place when they have turned positive for CD44 and negative for CD69 expression, i.e. at the stage when they prepare for their egress from pancreatic lymph nodes. Based on the RIP-LCMV model, the impact of the CXCR3/CXCL10 axis in autoimmune diabetes appeared first decisive [18, 19], but in a more recent study, the 1F11 antibody [56], used also in this present study, offered only marginal protection against diabetes development. In the model of cyclophosphamide-accelerated diabetes in NOD mice, the role of CXCL10 in T-cell chemo-attraction appeared redundant, although CXCL10 neutralization by antibody treatment inhibited diabetes development [57]. Rather than inhibiting lymphocyte accumulation, the treatment promoted beta cell regeneration, a phenomenon subsequently linked to detrimental effects of CXCL10 expression upon viability of beta cells [58]. The necessity of the CXCR3/CXCL10 axis in diabetes development was also challenged by a study reporting accelerated insulitis and diabetes development in NOD mice made congenic for a null-mutation in CXCR3 [59]. However, the absence of CXCR3 can induce other effects in addition to disrupting CXCL10-based recruitment to the islets and, as a genetic modification, is likely to interfere with developmental aspects of the immune system involved in T1D autoimmunity, leading to different outcomes. This is similar to the differences reported between TLR4-deficient NOD mice and NOD mice subjected to treatment with a TLR4 antagonist [47, 60].

Despite some variable results obtained with anti-CXCL10 antibody treatment, studies using the RIP-LCMV model and hyperglycemia reversal model with anti-CD3-treatment of diabetic NOD mice report clear therapeutic effects after neutralization of CXCL10 [61]. In the present study, we tested the therapeutic effect of CXCL10 neutralization on early T-cell recruitment in NOD mice with gut dysbiosis and focused on CXCL10 expression in their islets. Although not completely prevented, insulitis was inhibited significantly by neutralization of CXCL10. Importantly, neutralization of CXCL10 had a selective effect on recruitment of T cells (both CD4 and CD8 subsets), while it allowed B-cell recruitment to continue. Although B-cells do not express CXCL10, it is possible that the selective inhibition of T-cell recruitment may also indirectly alter the composition of numerous B-cell subsets present in islets[38]. The present study nevertheless corroborates a functional role for CXCL10 in T-cell recruitment in islets and provides relevance for anti-CXCL10 therapies as a potential intervention strategy to halt progression of T-cell recruitment arising from gut microbiota interactions with host immune system [9, 62] including LPS [63].

Macrophages are the only leukocytes present in islets at birth and persisting in the islets as NOD mice age [38, 64]. A subset likely arises from these resident macrophages and expresses a number of proinflammatory transcripts including chemokines *Cxcl9* and *Cxcl10* [27, 38]. Systemic administration of a small amount (100 ng) of LPS induces *Cxcl10* transcripts both in wild-type and *Rag1-/-* NOD mice [27], indicating that T cells are not an absolute prerequisite for induction of *Cxcl10* in islet-resident macrophages. We found that even a low concentration of LPS, corresponding to levels measured during metabolic endotoxemia [65], induced CXCL10 production in cultured islets of *Rag1-/-* and also of *IFNγr* -/- NOD mice; thus dissociating CXCL10 production in islets from the necessity of IFNγ and T cells. In cultured murine macrophages, *Cxcl10* transcripts are induced by LPS even at a relatively minute concentration (0.1 ng/ml) [44], indicating that CXCL10 expression in islets may be stimulated by LPS at levels well comparable to metabolic endotoxemia [65]. Consistent with the notion that islet-resident macrophages and macrophages in barrier tissues are adapted to sense microbial products

such as bacterial lipopolysaccharides in blood [27], we found that chemical depletion of macrophages in islets before stimulation with LPS strongly inhibited CXCL10 production.

Although depletion of macrophages impacted strongly on CXCL10 production in islets, CXCL10 can be induced in various non-immune cell types including keratinocytes, fibroblasts, astrocytes and endothelial cells [66]. Positive staining of endocrine cells islets for CXCL10 in immunohistochemistry of human and rodent islets [11, 14] suggests that endocrine cells may also produce CXCL10. NIT-1 cells produce CXCL10 transcripts in response to cytokine stimulation [19], but the potential of islet beta cells to produce CXCL10 and to respond to LPS was not previously addressed. In addition to macrophages [27], beta cells also express toll-like receptors including TLR4 [67], and as documented earlier [26], islet cells upregulate TLRs in response to LPS. We addressed the biological significance of TLR4 expression in beta cells by studying the transcriptome of beta cells purified from LPS-stimulated islets, and found upregulation of *Cxcl10* and other genes associated with the TLR4-signaling pathway. LPS also upregulated genes for inflammatory responses, including signaling pathways for type I interferon and TNF, along with upregulated genes for antigen processing and presentation of MHC class I molecules. Of the interferon-regulated transcription factors (IRF), LPS induced expression of *Irf1*, *Irf7* and *Irf9* in beta cells. In particular, IRF7 is implicated in mediating endotoxin-induced type I interferon production in macrophages [68]. The strong induction of IRF7 in beta cells may augment activation of the type I interferon signaling pathway in beta cells, conventionally attributed to infiltrating macrophages [69]. Activation of these identified pathways in beta cells may thus facilitate both the entry of autoimmune T cells in islets and the direct recognition of beta cells by autoimmune CD8 T cells. This suggests that LPS can prime also beta cells themselves for their eventual destruction.

Of the type I interferons, IFNβ can be induced by LPS [70, 71], whereas there is no evidence of IFNα being induced by LPS. The lack of CXCL10 production in islets of *Ifnar-/-* mice following LPS stimulation indicates that IFNβ is the likely key to type I-interferon-mediated LPS effect in islets, because *I*fnar-/- mice used in this study lack IFNAR1, which is required for signaling of both IFNA and IFNβ interferons

[72]. The ability of LPS to induce IFNβrelies on the MyD88-independent pathway of TLR4 signaling, and IRF3 is the key transcription factor mediating type I interferon production in response to LPS [73]. IRF7 may play a role downstream of IFNAR, as IFNβ induction in response to LPS abolished in *Ifnar1*-deficient murine macrophages, reportedly deficient also of IRF7 [68, 69]. Moreover, CXCL10 production in response to TNF strongly inhibited following macrophage depletion in islets. The CXCL10 promoter also contains a functional nuclear factor kappa B (NF-κB) element [46], which probably allows CXCL10 to be induced effectively in islet macrophages activated by a variety of TRAF-containing TNFSFR-receptors in addition to interferon receptors.

Although several mechanisms have been identified related to how gut microbiota and gut dysbiosis may intersect with islet-autoimmunity [74], the present study is perhaps the first to identify a sequence of innate immune mechanisms by which gut dysbiosis may make islets vulnerable to destruction by islet-autoantigen specific T cells. Our results pinpoint circulating endotoxin as an effector molecule that can induce production of CXCL10 chemokine by both islet macrophages and beta cells, and a type I interferon, IFNβ, being the mediator of this downstream endotoxin effect. The subsequent increase in local CXCL10 within the islets enhances the recruitment of T cells imprinted in PLN with CXCR3. T-cell activation in NOD mice has been shown to be preceded by a phase of type I interferon signature in islets [17]. Our study indicates that this may derive from dysbiosis-related endotoxemia, either alone or in synergy with other potential type I interferon-inducers to attract the earliest T cells in islets.

## Author contributions

Conceptualization: Arno Hänninen, Thomas Kay, Helen Thomas, Urs Christen and Andrew Luster. Methodology: Sakari Pöysti, Satu Silojärvi, Thomas Brodnicki, Helen Thomas, Xin Liu, Urs Christen and Andrew Luster. Investigation: Sakari Pöysti, Satu Silojärvi, Tara Catterall, Xin Liu and Leanne Mackin.

Writing – Original Draft: Arno Hänninen and Sakari Pöysti. Writing – Review & Editing: Sakari Pöysti, Satu Silojärvi, Thomas Brodnick, Helen Thomas, Urs Christen, Thomas Kay, Andrew Luster and Arno Hänninen. Resources, Andrew Luster and Urs Christen.

## Declaration of competing interest

The authors have declared that no conflict of interest exists.

## Acknowledgments

This work was funded by NovoNordisk Foundation (NNF18OC0033880), InFLAMES Flagship Programme of the Academy of Finland (#337530), State research funding for university level health research in Turku University Hospital, Instrumentarium Research Foundation (#200056), Emil Aaltonen foundation #210181; the National Health, Medical Research Council of Australia (NHMRC) (Program grants GNT1126237 and GNT1150425), and Landes-Offensive zur Entwicklung Wissenschaftlich-ökonomischer Exzellenz (LOEWE) Translational Medicine and Pharmacology (#TMP-IF-01). St Vincent's Institute receives support from the Operational Infrastructure Support Scheme of the Government of Victoria. We thank E. Pappas and S. Litwak for technical support, genotyping and animal husbandry. We also thank NIH tetramer facility (Emory University, Atlanta, GA) for providing antigen-MHC tetramers, and Turku Bioscience Cell Imaging and Cytometry Unit for the use of the equipment.

## Data availability statement

The datasets generated during the current study are available in the GEO repository. The authors declare that all other data supporting the findings of this study are available within the article and its supplemental material files. All biological materials except MHC-tetramers are available from common vendors (specified in Material and methods) or made available from the authors upon request.

## References


[1] K. M. Drescher, M. von Herrath, and S. Tracy, "Enteroviruses, hygiene and type 1 diabetes: toward a preventive vaccine," *Rev Med Virol,* vol. 25, pp. 19-32, Jan 2015.

[2] S. Tracy, K. M. Drescher, and N. M. Chapman, "Enteroviruses and type 1 diabetes," *Diabetes Metab Res Rev,* vol. 27, pp. 820-3, Nov 2011.

[3] N. M. Chapman, K. Coppieters, M. von Herrath, and S. Tracy, "The microbiology of human hygiene and its impact on type 1 diabetes," *Islets,* vol. 4, pp. 253-61, Jul-Aug 2012.

[4] E. E. Hamilton-Williams, G. L. Lorca, J. M. Norris, and J. L. Dunne, "A Triple Threat? The Role of Diet, Nutrition, and the Microbiota in T1D Pathogenesis," *Front Nutr,* vol. 8, p. 600756, 2021.

[5] H. Siljander, J. Honkanen, and M. Knip, "Microbiome and type 1 diabetes," *EBioMedicine,* vol. 46, pp. 512-521, Aug 2019.

[6] J. E. Harbison, A. J. Roth-Schulze, L. C. Giles, C. D. Tran, K. M. Ngui, M. A. Penno*, et al.*, "Gut microbiome dysbiosis and increased intestinal permeability in children with islet autoimmunity and type 1 diabetes: A prospective cohort study," *Pediatr Diabetes,* vol. 20, pp. 574-583, Aug 2019.

[7] M. Levy, A. A. Kolodziejczyk, C. A. Thaiss, and E. Elinav, "Dysbiosis and the immune system," *Nat Rev Immunol,* vol. 17, pp. 219-232, Apr 2017.

[8] J. E. Harbison, R. L. Thomson, J. M. Wentworth, J. Louise, A. Roth-Schulze, R. J. Battersby*, et al.*, "Associations between diet, the gut microbiome and short chain fatty acids in youth with islet autoimmunity and type 1 diabetes," *Pediatr Diabetes,* vol. 22, pp. 425-433, May 2021.

[9] T. Vatanen, E. A. Franzosa, R. Schwager, S. Tripathi, T. D. Arthur, K. Vehik*, et al.*, "The human gut microbiome in early-onset type 1 diabetes from the TEDDY study," *Nature,* vol. 562, pp. 589-594, Oct 2018.

[10] J. R. Groom and A. D. Luster, "CXCR3 in T cell function," *Exp Cell Res,* vol. 317, pp. 620-31, Mar 10 2011.

[11] A. Antonelli, S. M. Ferrari, A. Corrado, E. Ferrannini, and P. Fallahi, "CXCR3, CXCL10 and type 1 diabetes," *Cytokine Growth Factor Rev,* vol. 25, pp. 57-65, Feb 2014.

[12] F. Nicoletti, I. Conget, M. Di Mauro, R. Di Marco, M. C. Mazzarino, K. Bendtzen*, et al.*, "Serum concentrations of the interferon-gamma-inducible chemokine IP-10/CXCL10 are augmented in both newly diagnosed Type I diabetes mellitus patients and subjects at risk of developing the disease," *Diabetologia,* vol. 45, pp. 1107-10, Aug 2002.

[13] A. Shimada, J. Morimoto, K. Kodama, R. Suzuki, Y. Oikawa, O. Funae*, et al.*, "Elevated serum IP-10 levels observed in type 1 diabetes," *Diabetes Care,* vol. 24, pp. 510-5, Mar 2001.

[14] B. O. Roep, F. S. Kleijwegt, A. G. van Halteren, V. Bonato, U. Boggi, F. Vendrame*, et al.*, "Islet inflammation and CXCL10 in recent-onset type 1 diabetes," *Clin Exp Immunol,* vol. 159, pp. 338-43, Mar 2010.

[15] S. A. Sarkar, C. E. Lee, F. Victorino, T. T. Nguyen, J. A. Walters, A. Burrack*, et al.*, "Expression and regulation of chemokines in murine and human type 1 diabetes," *Diabetes,* vol. 61, pp. 436-46, Feb 2012.

[16] S. Uno, A. Imagawa, K. Saisho, K. Okita, H. Iwahashi, T. Hanafusa*, et al.*, "Expression of chemokines, CXC chemokine ligand 10 (CXCL10) and CXCR3 in the inflamed islets of patients with recent-onset autoimmune type 1 diabetes," *Endocr J,* vol. 57, pp. 991-6, 2010.

[17] J. A. Carrero, B. Calderon, F. Towfic, M. N. Artyomov, and E. R. Unanue, "Defining the transcriptional and cellular landscape of type 1 diabetes in the NOD mouse," *PLoS One,* vol. 8, p. e59701, 2013.

[18] U. Christen, D. B. McGavern, A. D. Luster, M. G. von Herrath, and M. B. Oldstone, "Among CXCR3 chemokines, IFN-gamma-inducible protein of 10 kDa (CXC chemokine ligand (CXCL)

10) but not monokine induced by IFN-gamma (CXCL9) imprints a pattern for the subsequent development of autoimmune disease," *J Immunol,* vol. 171, pp. 6838-45, Dec 15 2003.

[19] S. Frigerio, T. Junt, B. Lu, C. Gerard, U. Zumsteg, G. A. Hollander*, et al.*, "Beta cells are responsible for CXCR3-mediated T-cell infiltration in insulitis," *Nat Med,* vol. 8, pp. 1414-20, Dec 2002.

[20] A. M. Henschel, S. M. Cabrera, M. L. Kaldunski, S. Jia, R. Geoffrey, M. F. Roethle*, et al.*, "Modulation of the diet and gastrointestinal microbiota normalizes systemic inflammation and beta-cell chemokine expression associated with autoimmune diabetes susceptibility," *PLoS One,* vol. 13, p. e0190351, 2018.

[21] J. M. Schenkel and D. Masopust, "Tissue-resident memory T cells," *Immunity,* vol. 41, pp. 886-97, Dec 18 2014.

[22] C. Bender, T. Rodriguez-Calvo, N. Amirian, K. T. Coppieters, and M. G. von Herrath, "The healthy exocrine pancreas contains preproinsulin-specific CD8 T cells that attack islets in type 1 diabetes," *Sci Adv,* vol. 6, Oct 2020.

[23] H. Brauner, M. Elemans, S. Lemos, C. Broberger, D. Holmberg, M. Flodstrom-Tullberg*, et al.*, "Distinct phenotype and function of NK cells in the pancreas of nonobese diabetic mice," *J Immunol,* vol. 184, pp. 2272-80, Mar 1 2010.

[24] C. Bogdan and U. Schleicher, "Production of interferon-gamma by myeloid cells--fact or fancy?," *Trends Immunol,* vol. 27, pp. 282-90, Jun 2006.

[25] L. Darwich, G. Coma, R. Pena, R. Bellido, E. J. Blanco, J. A. Este*, et al.*, "Secretion of interferon-gamma by human macrophages demonstrated at the single-cell level after costimulation with interleukin (IL)-12 plus IL-18," *Immunology,* vol. 126, pp. 386-93, Mar 2009.

[26] L. Wen, J. Peng, Z. Li, and F. S. Wong, "The effect of innate immunity on autoimmune diabetes and the expression of Toll-like receptors on pancreatic islets," *J Immunol,* vol. 172, pp. 3173-80, Mar 1 2004.

[27] S. T. Ferris, P. N. Zakharov, X. Wan, B. Calderon, M. N. Artyomov, E. R. Unanue*, et al.*, "The islet-resident macrophage is in an inflammatory state and senses microbial products in blood," *J Exp Med,* vol. 214, pp. 2369-2385, Aug 7 2017.

[28] P. D. Cani, R. Bibiloni, C. Knauf, A. Waget, A. M. Neyrinck, N. M. Delzenne*, et al.*, "Changes in gut microbiota control metabolic endotoxemia-induced inflammation in high-fat diet-induced obesity and diabetes in mice," *Diabetes,* vol. 57, pp. 1470-81, Jun 2008.

[29] M. T. Henke, D. J. Kenny, C. D. Cassilly, H. Vlamakis, R. J. Xavier, and J. Clardy, "Ruminococcus gnavus, a member of the human gut microbiome associated with Crohn's disease, produces an inflammatory polysaccharide," *Proc Natl Acad Sci U S A,* vol. 116, pp. 12672-12677, Jun 25 2019.

[30] J. W. Collins, K. M. Keeney, V. F. Crepin, V. A. Rathinam, K. A. Fitzgerald, B. B. Finlay*, et al.*, "Citrobacter rodentium: infection, inflammation and the microbiota," *Nat Rev Microbiol,* vol. 12, pp. 612-23, Sep 2014.

[31] T. Rahman, A. S. Brown, E. L. Hartland, I. R. van Driel, and K. Y. Fung, "Plasmacytoid Dendritic Cells Provide Protection Against Bacterial-Induced Colitis," *Front Immunol,* vol. 10, p. 608, 2019.

[32] S. Poysti, S. Silojarvi, R. Toivonen, and A. Hanninen, "Plasmacytoid dendritic cells regulate host immune response to Citrobacter rodentium induced colitis in colon-draining lymph nodes," *Eur J Immunol,* vol. 51, pp. 620-625, Mar 2021.

[33] K. L. Graham, S. Fynch, E. G. Papas, C. Tan, T. W. H. Kay, and H. E. Thomas, "Isolation and Culture of the Islets of Langerhans from Mouse Pancreas," *Bio-protocol,* vol. 6, p. e1840, 2016/06/20 2016.

[34] P. Bonvin, F. Gueneau, V. Buatois, M. Charreton-Galby, S. Lasch, M. Messmer*, et al.*, "Antibody Neutralization of CXCL10 in Vivo Is Dependent on Binding to Free and Not Endothelial-bound Chemokine: IMPLICATIONS FOR THE DESIGN OF A NEW GENERATION OF

ANTI-CHEMOKINE THERAPEUTIC ANTIBODIES," *J Biol Chem,* vol. 292, pp. 4185-4197, Mar 10 2017.

[35] I. A. Khan, J. A. MacLean, F. S. Lee, L. Casciotti, E. DeHaan, J. D. Schwartzman*, et al.*, "IP-10 is critical for effector T cell trafficking and host survival in Toxoplasma gondii infection," *Immunity,* vol. 12, pp. 483-94, May 2000.

[36] U. Christen and R. Kimmel, "Chemokines as Drivers of the Autoimmune Destruction in Type 1 Diabetes: Opportunity for Therapeutic Intervention in Consideration of an Optimal Treatment Schedule," *Front Endocrinol (Lausanne),* vol. 11, p. 591083, 2020.

[37] S. Poysti, R. Toivonen, A. Takeda, S. Silojarvi, E. Yatkin, M. Miyasaka*, et al.*, "Infection with the enteric pathogen C. rodentium promotes islet-specific autoimmunity by activating a lymphatic route from the gut to pancreatic lymph node," *Mucosal Immunol,* vol. 15, pp. 471-479, Mar 2022.

[38] P. N. Zakharov, H. Hu, X. Wan, and E. R. Unanue, "Single-cell RNA sequencing of murine islets shows high cellular complexity at all stages of autoimmune diabetes," *J Exp Med,* vol. 217, Jun 1 2020.

[39] J. A. Mullaney, J. E. Stephens, M. E. Costello, C. Fong, B. E. Geeling, P. G. Gavin*, et al.*, "Type 1 diabetes susceptibility alleles are associated with distinct alterations in the gut microbiota," *Microbiome,* vol. 6, p. 35, Feb 17 2018.

[40] J. R. Mora, M. R. Bono, N. Manjunath, W. Weninger, L. L. Cavanagh, M. Rosemblatt*, et al.*, "Selective imprinting of gut-homing T cells by Peyer's patch dendritic cells," *Nature,* vol. 424, pp. 88-93, Jul 3 2003.

[41] L. Marroqui, R. S. Dos Santos, A. Op de Beeck, A. Coomans de Brachene, L. Marselli, P. Marchetti*, et al.*, "Interferon-alpha mediates human beta cell HLA class I overexpression, endoplasmic reticulum stress and apoptosis, three hallmarks of early human type 1 diabetes," *Diabetologia,* vol. 60, pp. 656-667, Apr 2017.

[42] Y. Ohmori and T. A. Hamilton, "Cooperative interaction between interferon (IFN) stimulus response element and kappa B sequence motifs controls IFN gamma- and lipopolysaccharide-stimulated transcription from the murine IP-10 promoter," *J Biol Chem,* vol. 268, pp. 6677-88, Mar 25 1993.

[43] V. Toshchakov, B. W. Jones, P. Y. Perera, K. Thomas, M. J. Cody, S. Zhang*, et al.*, "TLR4, but not TLR2, mediates IFN-beta-induced STAT1alpha/beta-dependent gene expression in macrophages," *Nat Immunol,* vol. 3, pp. 392-8, Apr 2002.

[44] L. M. Kanevskiy, W. G. Telford, A. M. Sapozhnikov, and E. I. Kovalenko, "Lipopolysaccharide induces IFN-gamma production in human NK cells," *Front Immunol,* vol. 4, p. 11, 2013.

[45] J. A. Carrero, D. P. McCarthy, S. T. Ferris, X. Wan, H. Hu, B. H. Zinselmeyer*, et al.*, "Resident macrophages of pancreatic islets have a seminal role in the initiation of autoimmune diabetes of NOD mice," *Proc Natl Acad Sci U S A,* vol. 114, pp. E10418-E10427, Nov 28 2017.

[46] J. R. Groom and A. D. Luster, "CXCR3 ligands: redundant, collaborative and antagonistic functions," *Immunol Cell Biol,* vol. 89, pp. 207-15, Feb 2011.

[47] E. Gulden, M. Ihira, A. Ohashi, A. L. Reinbeck, M. A. Freudenberg, H. Kolb*, et al.*, "Toll-like receptor 4 deficiency accelerates the development of insulin-deficient diabetes in non-obese diabetic mice," *PLoS One,* vol. 8, p. e75385, 2013.

[48] M. C. Simon, A. L. Reinbeck, C. Wessel, J. Heindirk, T. Jelenik, K. Kaul*, et al.*, "Distinct alterations of gut morphology and microbiota characterize accelerated diabetes onset in nonobese diabetic mice," *J Biol Chem,* vol. 295, pp. 969-980, Jan 24 2020.

[49] M. P. Burrows, P. Volchkov, K. S. Kobayashi, and A. V. Chervonsky, "Microbiota regulates type 1 diabetes through Toll-like receptors," *Proc Natl Acad Sci U S A,* vol. 112, pp. 9973-7, Aug 11 2015.

[50] J. Tian, D. Zekzer, L. Hanssen, Y. Lu, A. Olcott, and D. L. Kaufman, "Lipopolysaccharide-activated B cells down-regulate Th1 immunity and prevent autoimmune diabetes in nonobese diabetic mice," *J Immunol,* vol. 167, pp. 1081-9, Jul 15 2001.

[51] A. S. Lee, D. L. Gibson, Y. Zhang, H. P. Sham, B. A. Vallance, and J. P. Dutz, "Gut barrier disruption by an enteric bacterial pathogen accelerates insulitis in NOD mice," *Diabetologia,* vol. 53, pp. 741-8, Apr 2010.

[52] E. Bosi, L. Molteni, M. G. Radaelli, L. Folini, I. Fermo, E. Bazzigaluppi*, et al.*, "Increased intestinal permeability precedes clinical onset of type 1 diabetes," *Diabetologia,* vol. 49, pp. 2824-7, Dec 2006.

[53] A. Sapone, L. de Magistris, M. Pietzak, M. G. Clemente, A. Tripathi, F. Cucca*, et al.*, "Zonulin upregulation is associated with increased gut permeability in subjects with type 1 diabetes and their relatives," *Diabetes,* vol. 55, pp. 1443-9, May 2006.

[54] F. R. Costa, M. C. Francozo, G. G. de Oliveira, A. Ignacio, A. Castoldi, D. S. Zamboni*, et al.*, "Gut microbiota translocation to the pancreatic lymph nodes triggers NOD2 activation and contributes to T1D onset," *J Exp Med,* vol. 213, pp. 1223-39, Jun 27 2016.

[55] S. J. Turley, J. W. Lee, N. Dutton-Swain, D. Mathis, and C. Benoist, "Endocrine self and gut non-self intersect in the pancreatic lymph nodes," *Proc Natl Acad Sci U S A,* vol. 102, pp. 17729-33, Dec 6 2005.

[56] K. T. Coppieters, N. Amirian, P. P. Pagni, C. Baca Jones, A. Wiberg, S. Lasch*, et al.*, "Functional redundancy of CXCR3/CXCL10 signaling in the recruitment of diabetogenic cytotoxic T lymphocytes to pancreatic islets in a virally induced autoimmune diabetes model," *Diabetes,* vol. 62, pp. 2492-9, Jul 2013.

[57] J. Morimoto, H. Yoneyama, A. Shimada, T. Shigihara, S. Yamada, Y. Oikawa*, et al.*, "CXC chemokine ligand 10 neutralization suppresses the occurrence of diabetes in nonobese diabetic mice through enhanced beta cell proliferation without affecting insulitis," *J Immunol,* vol. 173, pp. 7017-24, Dec 1 2004.

[58] F. T. Schulthess, F. Paroni, N. S. Sauter, L. Shu, P. Ribaux, L. Haataja*, et al.*, "CXCL10 impairs beta cell function and viability in diabetes through TLR4 signaling," *Cell Metab,* vol. 9, pp. 125-39, Feb 2009.

[59] Y. Yamada, Y. Okubo, A. Shimada, Y. Oikawa, S. Yamada, S. Narumi*, et al.*, "Acceleration of diabetes development in CXC chemokine receptor 3 (CXCR3)-deficient NOD mice," *Diabetologia,* vol. 55, pp. 2238-45, Aug 2012.

[60] M. Alibashe-Ahmed, E. Brioudes, W. Reith, D. Bosco, and T. Berney, "Toll-like receptor 4 inhibition prevents autoimmune diabetes in NOD mice," *Sci Rep,* vol. 9, p. 19350, Dec 18 2019.

[61] S. Lasch, P. Muller, M. Bayer, J. M. Pfeilschifter, A. D. Luster, E. Hintermann*, et al.*, "Anti-CD3/Anti-CXCL10 Antibody Combination Therapy Induces a Persistent Remission of Type 1 Diabetes in Two Mouse Models," *Diabetes,* vol. 64, pp. 4198-211, Dec 2015.

[62] C. J. Stewart, N. J. Ajami, J. L. O'Brien, D. S. Hutchinson, D. P. Smith, M. C. Wong*, et al.*, "Temporal development of the gut microbiome in early childhood from the TEDDY study," *Nature,* vol. 562, pp. 583-588, Oct 2018.

[63] T. Vatanen, A. D. Kostic, E. d'Hennezel, H. Siljander, E. A. Franzosa, M. Yassour*, et al.*, "Variation in Microbiome LPS Immunogenicity Contributes to Autoimmunity in Humans," *Cell,* vol. 165, pp. 842-53, May 5 2016.

[64] B. Calderon, J. A. Carrero, S. T. Ferris, D. K. Sojka, L. Moore, S. Epelman*, et al.*, "The pancreas anatomy conditions the origin and properties of resident macrophages," *J Exp Med,* vol. 212, pp. 1497-512, Sep 21 2015.

[65] P. D. Cani, J. Amar, M. A. Iglesias, M. Poggi, C. Knauf, D. Bastelica*, et al.*, "Metabolic endotoxemia initiates obesity and insulin resistance," *Diabetes,* vol. 56, pp. 1761-72, Jul 2007.

[66] M. Metzemaekers, V. Vanheule, R. Janssens, S. Struyf, and P. Proost, "Overview of the Mechanisms that May Contribute to the Non-Redundant Activities of Interferon-Inducible CXC Chemokine Receptor 3 Ligands," *Front Immunol,* vol. 8, p. 1970, 2017.

[67] C. Westwell-Roper, D. Nackiewicz, M. Dan, and J. A. Ehses, "Toll-like receptors and NLRP3 as central regulators of pancreatic islet inflammation in type 2 diabetes," *Immunol Cell Biol,* vol. 92, pp. 314-23, Apr 2014.

[68] W. X. Sin, J. P. Yeong, T. J. F. Lim, I. H. Su, J. E. Connolly, and K. C. Chin, "IRF-7 Mediates Type I IFN Responses in Endotoxin-Challenged Mice," *Front Immunol,* vol. 11, p. 640, 2020.

[69] S. Ning, J. S. Pagano, and G. N. Barber, "IRF7: activation, regulation, modification and function," *Genes Immun,* vol. 12, pp. 399-414, Sep 2011.

[70] N. A. de Weerd, J. P. Vivian, T. K. Nguyen, N. E. Mangan, J. A. Gould, S. J. Braniff*, et al.*, "Structural basis of a unique interferon-beta signaling axis mediated via the receptor IFNAR1," *Nat Immunol,* vol. 14, pp. 901-7, Sep 2013.

[71] S. Gessani, F. Belardelli, A. Pecorelli, P. Puddu, and C. Baglioni, "Bacterial lipopolysaccharide and gamma interferon induce transcription of beta interferon mRNA and interferon secretion in murine macrophages," *J Virol,* vol. 63, pp. 2785-9, Jun 1989.

[72] C. T. Ng, J. L. Mendoza, K. C. Garcia, and M. B. Oldstone, "Alpha and Beta Type 1 Interferon Signaling: Passage for Diverse Biologic Outcomes," *Cell,* vol. 164, pp. 349-52, Jan 28 2016.

[73] K. Honda and T. Taniguchi, "IRFs: master regulators of signalling by Toll-like receptors and cytosolic pattern-recognition receptors," *Nat Rev Immunol,* vol. 6, pp. 644-58, Sep 2006.

[74] P. G. Gavin and E. E. Hamilton-Williams, "The gut microbiota in type 1 diabetes: friend or foe?," *Curr Opin Endocrinol Diabetes Obes,* vol. 26, pp. 207-212, Aug 2019.

## Figure Legends

**Figure 1**: Dysbiosis increases gut leakiness in NOD mice and promotes CXCL10 expression in pancreatic islets. Haptoglobin (A) and LBP (B) levels in serum, and (C, D) CXCL10 expression in islets (Green=CXCL10) 7 days after dysbiosis induction with *C. rodentium* or *R. gnavus*. (E, F) Level of insulitis 14 days after dysbiosis induction. (G) Acceleration of diabetes development following dysbiosis induction with *C. rodentium* (n=21 per group). Each data point represents one mouse. Data are from three independent experiments, all mice were female NOD mice. In G, the difference in cumulative diabetes incidence is significant at week 14 and non-significant at week 19. Unpaired two-sided Student's t-test, *p*<0,05; p**<0,01; p***<0,001*. See also Figure S1.

**Figure 2.** Induction of CXCL10 by LPS *in vivo* and *in vitro* without and with IFNγ. (A) CXCL10 expression in islets after intraperitoneal injection of LPS (30 µg). (B) Induction of CXCL10 in C57BL/6 mice by intraperitoneal LPS. (C) *In vitro* LPS stimulation of cultured islets from young NOD donor mice with or without IFNγ (Mean + SEM). (D) Dose-response of CXCL10-induction by LPS in cultured islets. In A-B, each data point represents one mouse. In A-C, data are from three independent experiments, and in D, from additional 4 independent experiments. In (A) p-values were calculated by one-way ANOVA with Dunnett's multiple comparison. In (B) p-values were calculated by one-way ANOVA with Tukey's multiple comparison and in (C, D), with unpaired two-sided Student's t-test, p*<0,05; p**<0,01; p***<0,001; p****<0,0001

**Figure 3.** CXCL10 induction by dysbiosis depends on TLR4. (A) Daily treatment with TLR4 blocker TAK-242 inhibits CXCL10 induction in the islets of *C. rodentium*-treated NOD mice. (B) Administration of *C. rodentium* to TLR4-KO mice compared to untreated TLR-KO mice and wild-type C57BL/6 mice. (C) CXCL10 expression in islets of TLR-KO mice following direct injection of LPS (30µg i.p.). Each data point represents one mouse. Data are from three independent experiments. In (A, B), p-values were

calculated with one-way ANOVA with Tukey's multiple comparison, and in (C), with unpaired two-sided Student's t-test, p*<0,05; p***<0,001; p****<0,0001.

**Figure 4.** Dysbiosis promotes activation of islet-specific T cells and their CXCR3 expression. Flow cytometry analysis of PLN-derived CD45+/TCRβ+/CD8+ cells specific for Insulin (A) and IGRP (B) tetramer without and after C. rodentium –treatment (for representative dot-plots, see Suppl. Figures; dotted line represents LO91-99 control –tetramer level). (C, D) Expression of CXCR3 on IGRP-tetramer positive and negative CD8+ cells in the PLN. (E) Representative dot plots of activation markers CD44 and CD69 in CD8 cells in the PLN. (F) Activated CD44+/CD69- IGRP-reactive 8.3 T cells in the PLN after C. rodentium -treatment compared to control group. (G) Expression of CXCR3 in 8.3 T cells according to their expression of CD44 and CD69 in the PLN. (H) CXCR3 expression in activated (CD44+/CD69-) cells in the PLN as compared to the brachial lymph node (BLN). Each data point represents one mouse. Data are from 3-4 independent experiments. Unpaired two-sided Student's t-test, p*<0,05; p***<0,001; p****<0,0001 (B,D,F) and one-way ANOVA with Tukey's multiple comparison (G). IGRP-reactive T cells in transgenic 8.3NOD mice were gated as CD45+/TCRβ+/CD8+ cells (E,F). See also Figure S3.

**Figure 5**. CXCL10 mediates insulitis development and T-cell trafficking to pancreatic islets during dysbiosis. (A, B) Level of insulitis in NOD mice dysbiotic after *C. rodentium*-treatment and the effect of anti-CXCL10 antibody (1F11) on insulitis. (C) Representative staining of CD4 and CD8 T cells, and of CD19 B cells in islets compared to $CD45^+$ cells. Intensity of CD4 (D) and CD8 (E) cell-staining in islets relative to staining of CD19 cells. Each data point represents one mouse. Pancreas sections were stained with a cocktail of all 4 antibodies, and the quantifications of CD4 and CD8 in relation to CD19 were done for the same set of islets. Intensities were quantitated using ImageJ software and expressed as arbitrary units (AU). A minimum of 20 islets were analyzed in each mouse. Data are from two independent experiments. Unpaired two-sided Student's t-test, *p*<0,05; p***<0,001*

**Figure 6.** Induction of CXCL10 in pancreatic islets lacking T cells or IFNγ- or type I IFN-receptor signaling, the effect of myeloid-cell depletion by clodronate, and the effect of interferon receptors in CXC10 induction in islets *in vivo* in wild-type and receptor-deficient NOD mice**.** (A) CXCL10 production in RAG-KO islets, and (B) in IFNGR-KO islets after stimulation with LPS and IFNγ. (C) CXCL10 expression in islets in mice deficient of IFNGR- or IFNAR1-receptor or three receptors (including IFNL-receptor; "triple KO") following LPS injection. (D) Effect of IFNAR1-deficiency on CXCL10 induction in islets treated with LPS and IFNγ. (E) Effect of myeloid-cell depletion by clodronate on induction of CXCL10 by LPS, TNF and IFNγ in wild type (left) and IFNGR-KO islets (right). Data are from three (A,B,D) and two (E) independent experiments of islets from 9 (A,B,D) and 5 (E) individual mice in each genotype (Mean ± SEM). In (E), islets were pretreated with clodronate (clod) or left untreated (nil) before stimulations with LPS (10 ng/ml) and/or indicated cytokine. Unpaired two-sided Student's t-test, *p*<0,05; p**<0,01*; *p***<0,001; p****<0,0001*. In (C), data are from 3 independent experiments, each data point representing one mouse. LPS was given in a dose of 30 µg. In (C, E) p-values were calculated with one-way ANOVA with Dunnett's multiple comparison.

**Figure 7.** Transcriptome analysis of β-cells isolated from whole islets cultured with or without LPS for 48 hours (n=5 independent samples/group). (A) Volcano plot showing genes highly expressed after culturing in media with LPS (red, log2 fold change>0) or without LPS (blue, log2 fold change<0). The top 30 differentially expressed genes (based on adjusted p value) and *Cxcl10* are labeled. (B) Gene ontology pathway analysis of genes upregulated in LPS-treated β-cells compared to control β-cells. The enrichment plot shows selected KEGG and REAC pathways with -log10 adjusted p value. (C) Heatmap of 35 selected genes upregulated in LPS-treated β-cells and have a role in cytokine-signaling pathways as defined by the KEGG and REEAC pathways shown in (B). (D) Real-time PCR expression of *Cxcl10* in untreated and LPS-stimulated β-cells. dCT represents the differential between *Cxcl10* and housekeeping gene (*β-actin*) in amplification cycle values giving threshold positivity (BMDM = bone-

marrow derived macrophages). Each data point represents β-cells from an individual Rag-deficient NOD mouse sorted in two independent experiments. Unpaired two-sided Student's t-test, *p****<0,0001*.

## Figures

Figure 1

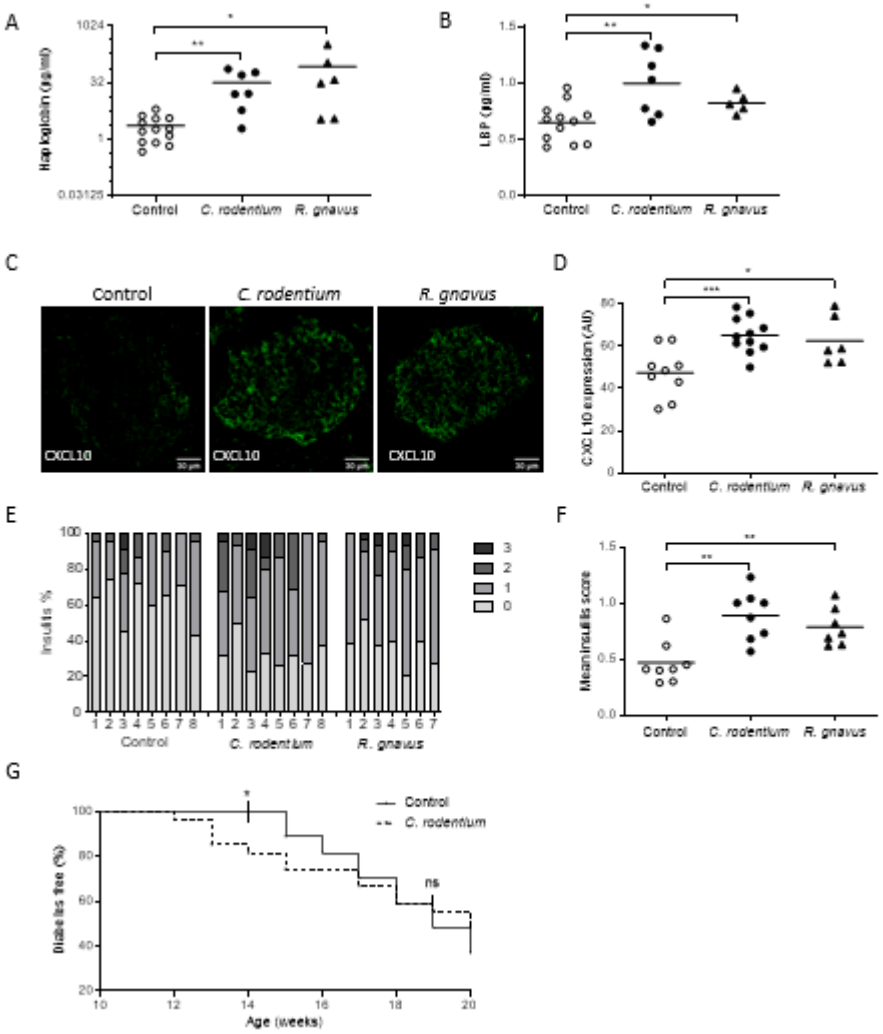


**Figure 1**: Dysbiosis increases gut leakiness in NOD mice and promotes CXCL10 expression in pancreatic islets. Haptoglobin (A) and LBP (B) levels in serum, and (C, D) CXCL10 expression in islets (Green=CXCL10) 7 days after dysbiosis induction with *C. rodentium* or *R. gnavus*. (E, F) Level of insulitis 14 days after dysbiosis induction. (G) Acceleration of diabetes development following dysbiosis induction with *C. rodentium* (n=21 per group). Each data point represents one mouse. Data are from 3 independent experiments.NOD mice were all females in each experiment In G, the difference in cumulative diabetes incidence is significant at week 14 (ns=non-significant). Unpaired two-sided Student's t-test, *p*<0,05; p**<0,01; p***<0,001*. See also Figure S1.

Figure 2

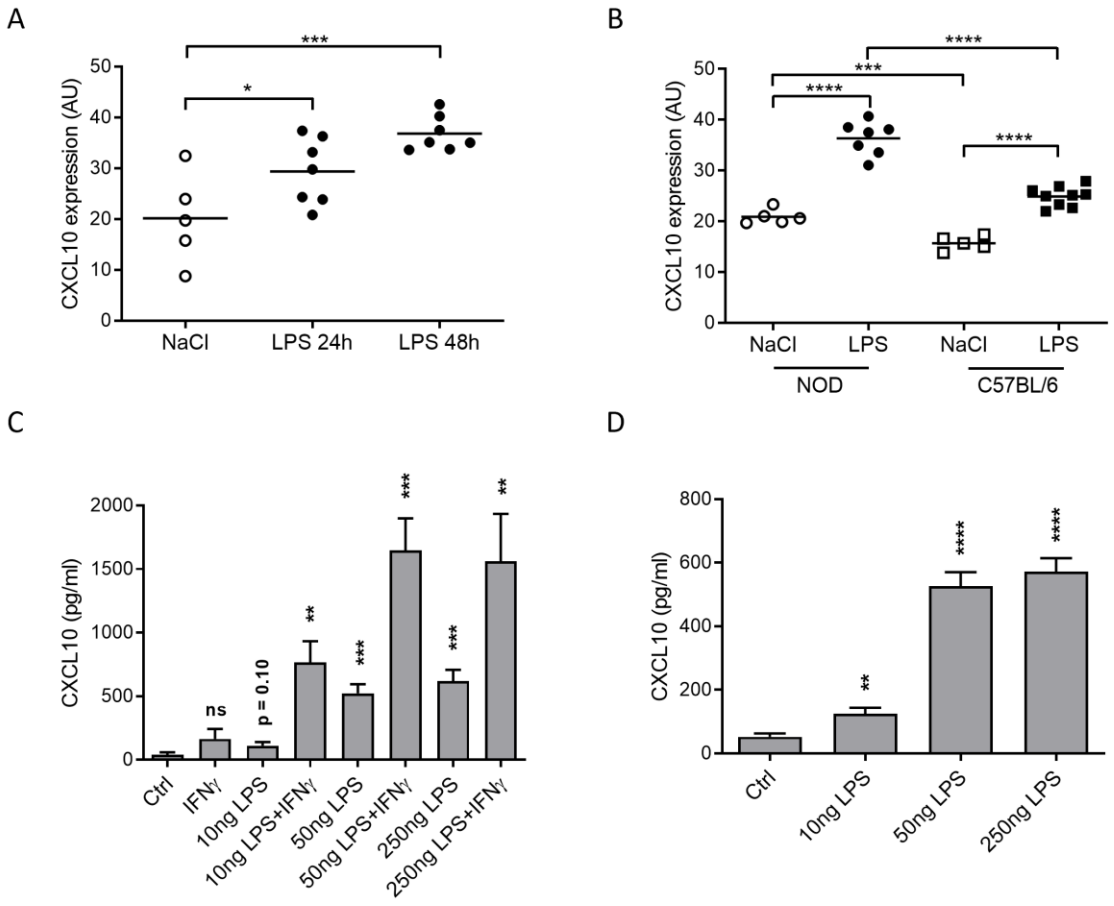


**Figure 2.** Induction of CXCL10 by LPS *in vivo* and *in vitro* without and with IFN-γ. (A) CXCL10 expression in islets after intraperitoneal injection of LPS (30 µg). (B) Induction of CXCL10 in C57BL/6 mice by intraperitoneal LPS. (C) *In vitro* LPS stimulation of cultured islets from young NOD donor mice with or without IFNγ (Mean + SEM). (D) Dose-response of CXCL10-induction by LPS in cultured islets. In A-B, each data point represents one mouse. In A-C, data are from three independent experiments, and in D, from additional 4 independent experiments. In (A) p-values were calculated by one-way ANOVA with Dunnett's multiple comparison. In (B) p-values were calculated by one-way ANOVA with Tukey's multiple comparison and in (C, D), with unpaired two-sided Student's t-test, p*<0,05; p**<0,01; p***<0,001; p****<0,0001

Figure 3

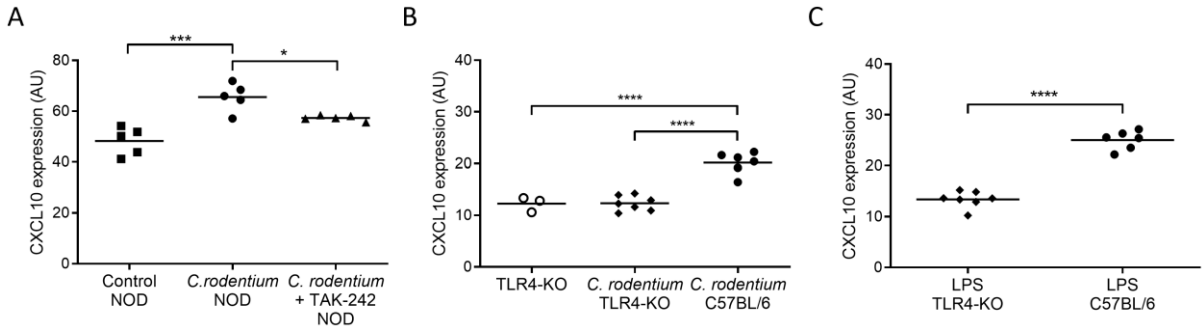


**Figure 3.** CXCL10 induction by dysbiosis depends on TLR4. (A) Daily treatment with TLR4 blocker TAK-242 inhibits CXCL10 induction in the islets of *C. rodentium*-treated NOD mice. (B) Administration of *C. rodentium* to TLR4-KO mice compared to untreated TLR-KO mice and wild-type C57BL/6 mice. (C) CXCL10 expression in islets of TLR-KO mice following direct injection of LPS (30µg i.p.). Each data point represents one mouse. Data are from three independent experiments. In (A, B), p-values were calculated with one-way ANOVA with Tukey's multiple comparison, and in (C), with unpaired two-sided Student's t-test, p*<0,05; p***<0,001; p****<0,0001.

Figure 4

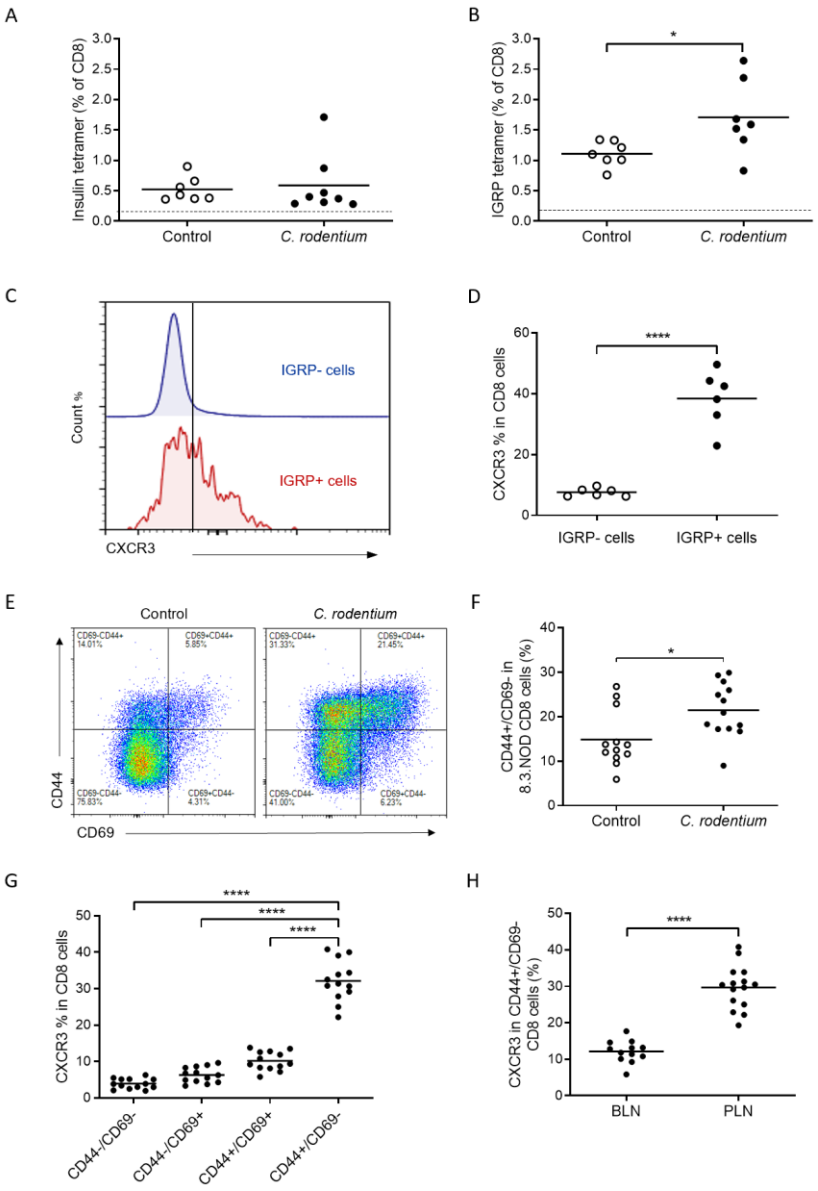


**Figure 4.** Dysbiosis promotes activation of islet-specific T cells and their CXCR3 expression. Flow cytometry analysis of PLN-derived CD45+/TCRβ+/CD8+ cells specific for Insulin (A) and IGRP (B) tetramer without and after C. rodentium –treatment (for representative dot-plots, see Suppl. Figures; dotted line represents LO91-99 control –tetramer level). (C, D) Expression of CXCR3 on IGRP-tetramer positive and negative CD8+ cells in the PLN. (E) Representative dot plots of activation markers CD44 and CD69 in CD8 cells in the PLN. (F) Activated CD44+/CD69- IGRP-reactive 8.3 T cells in the PLN after C. rodentium -treatment compared to control group. (G) Expression of CXCR3 in 8.3 T cells according to their expression of CD44 and CD69 in the PLN. (H) CXCR3 expression in activated (CD44+/CD69-) cells in the PLN as compared to the brachial lymph node (BLN). Each data point represents one mouse. Data are from 3-4 independent experiments. Unpaired two-sided Student's t-test, p*<0,05; p***<0,001; p****<0,0001 (B,D,F) and one-way ANOVA with Tukey's multiple comparison (G). IGRP-reactive T cells in transgenic 8.3NOD mice were gated as CD45+/TCRβ+/CD8+ cells (E,F). See also Figure S3.

Figure 5

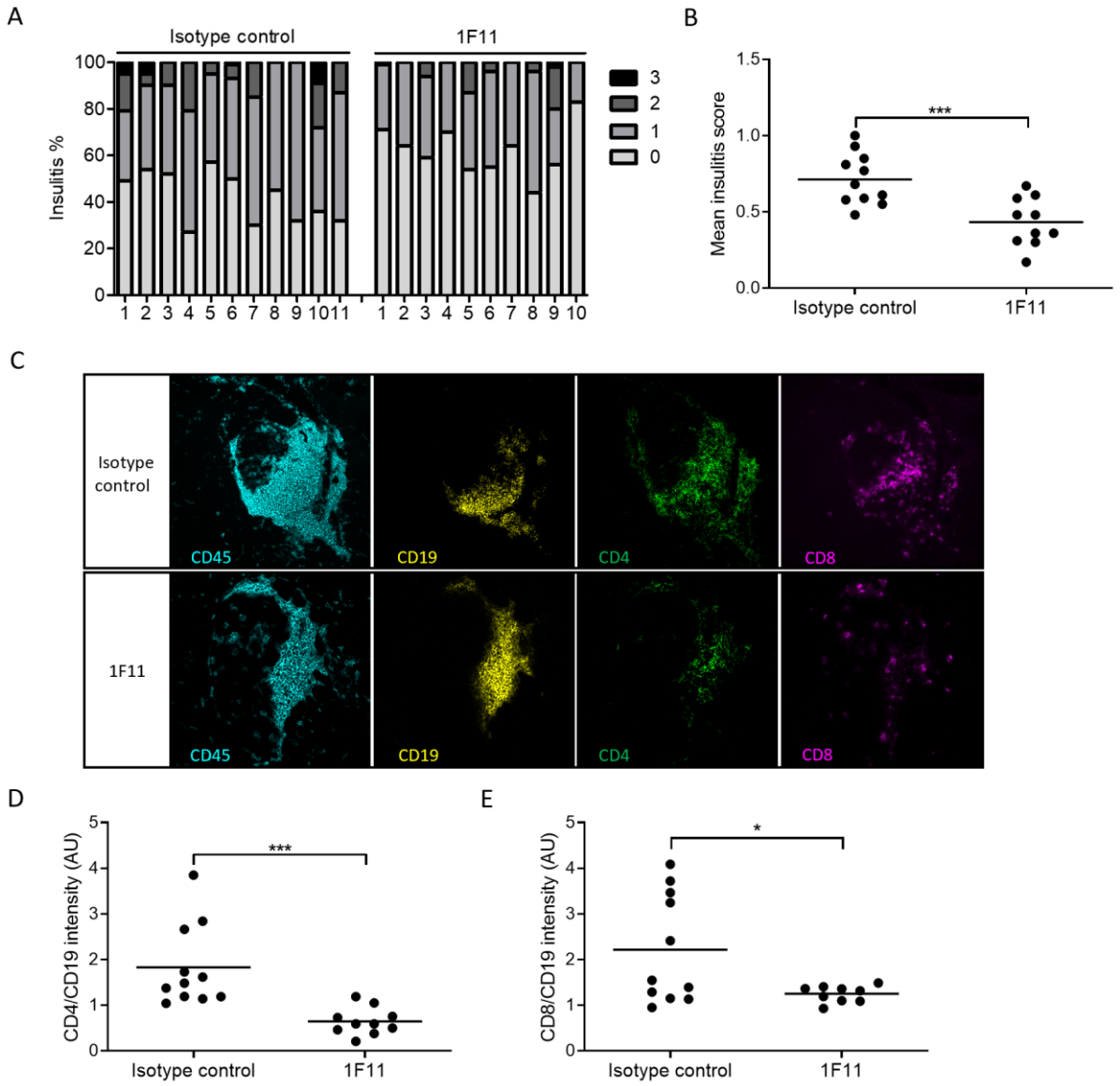


**Figure 5**. CXCL10 mediates insulitis development and T-cell trafficking to pancreatic islets during dysbiosis. (A, B) Level of insulitis in NOD mice dysbiotic after *C. rodentium*-treatment and the effect of anti-CXCL10 antibody (1F11) on insulitis. (C) Representative staining of CD4 and CD8 T cells, and of CD19 B cells in islets compared to $CD45^{+}$ cells. Intensity of CD4 (D) and CD8 (E) cell-staining in islets relative to staining of CD19 cells. Each data point represents one mouse. Pancreas sections were stained with a cocktail of all 4 antibodies, and the quantifications of CD4 and CD8 in relation to CD19 were done for the same set of islets. Intensities were quantitated using ImageJ software and expressed as arbitrary units (AU). A minimum of 20 islets were analyzed in each mouse. Data are from two independent experiments. Unpaired two-sided Student's t-test, *p*<0,05; p***<0,001*

Figure 6

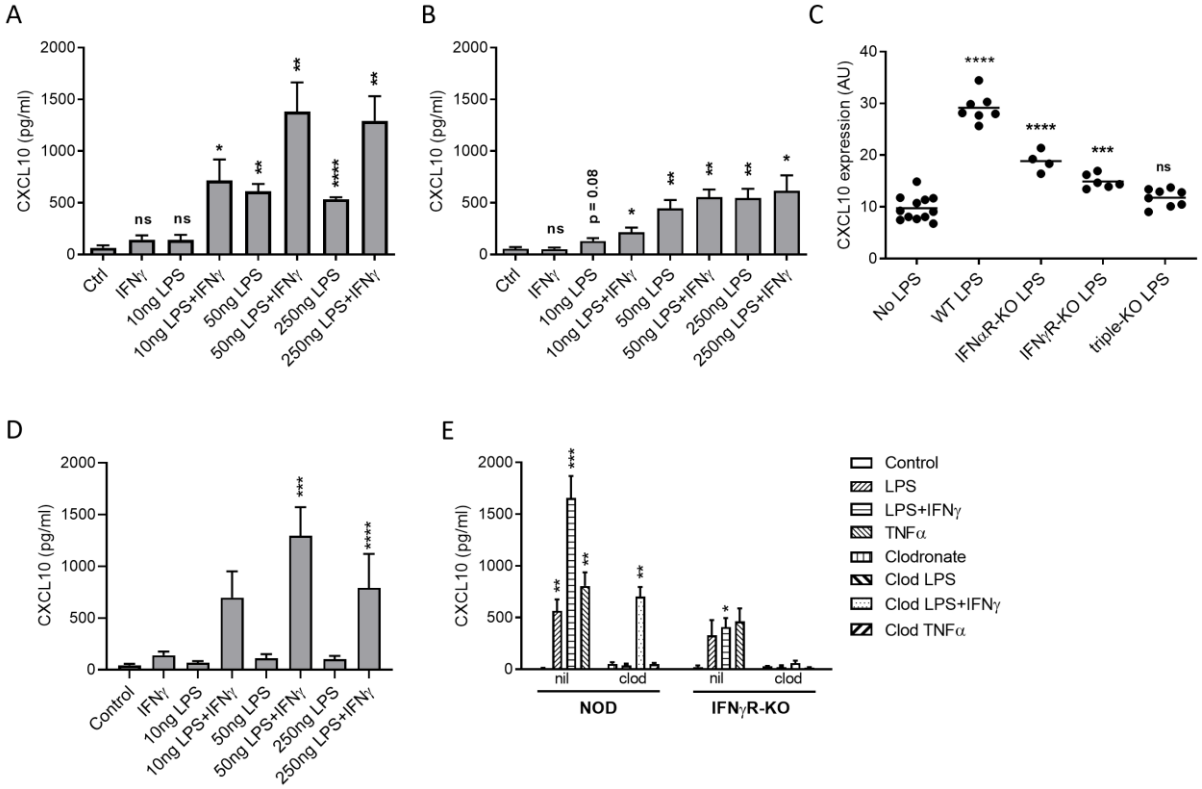


**Figure 6.** Induction of CXCL10 in pancreatic islets lacking T cells or IFNγ- or type I IFN-receptor signaling, the effect of myeloid-cell depletion by clodronate, and the effect of interferon receptors in CXC10 induction in islets *in vivo* in wild-type and receptor-deficient NOD mice**.** (A) CXCL10 production in RAG-KO islets, and (B) in IFNGR-KO islets after stimulation with LPS and IFNγ. (C) CXCL10 expression in islets in mice deficient of IFNγ- or IFNAR1-receptor or three receptors (including IFNL-receptor; "triple KO") following LPS injection. (D) Effect of IFNAR1-deficiency on CXCL10 induction in islets treated with LPS and IFNγ. (E) Effect of myeloid-cell depletion by clodronate on induction of CXCL10 by LPS, TNF and IFNγ in wild type (left) and IFNGR-KO islets (right). Data are from three (A,B,D) and two (E) independent experiments of islets from 9 (A,B,D) and 5 (E) individual mice in each genotype (Mean ± SEM). In (E), islets were pretreated with clodronate (clod) or left untreated (nil) before stimulations with LPS (10 ng/ml) and/or indicated cytokine. In (A, B) unpaired two-sided Student's t-test, *p*<0,05; p**<0,01*; *p***<0,001; p****<0,0001*. In (C), data are from 3 independent experiments, each data point representing one mouse. LPS was given in a dose of 30 µg. In (C-E) p-values were calculated with one-way ANOVA with Dunnett's multiple comparison.

Figure 7

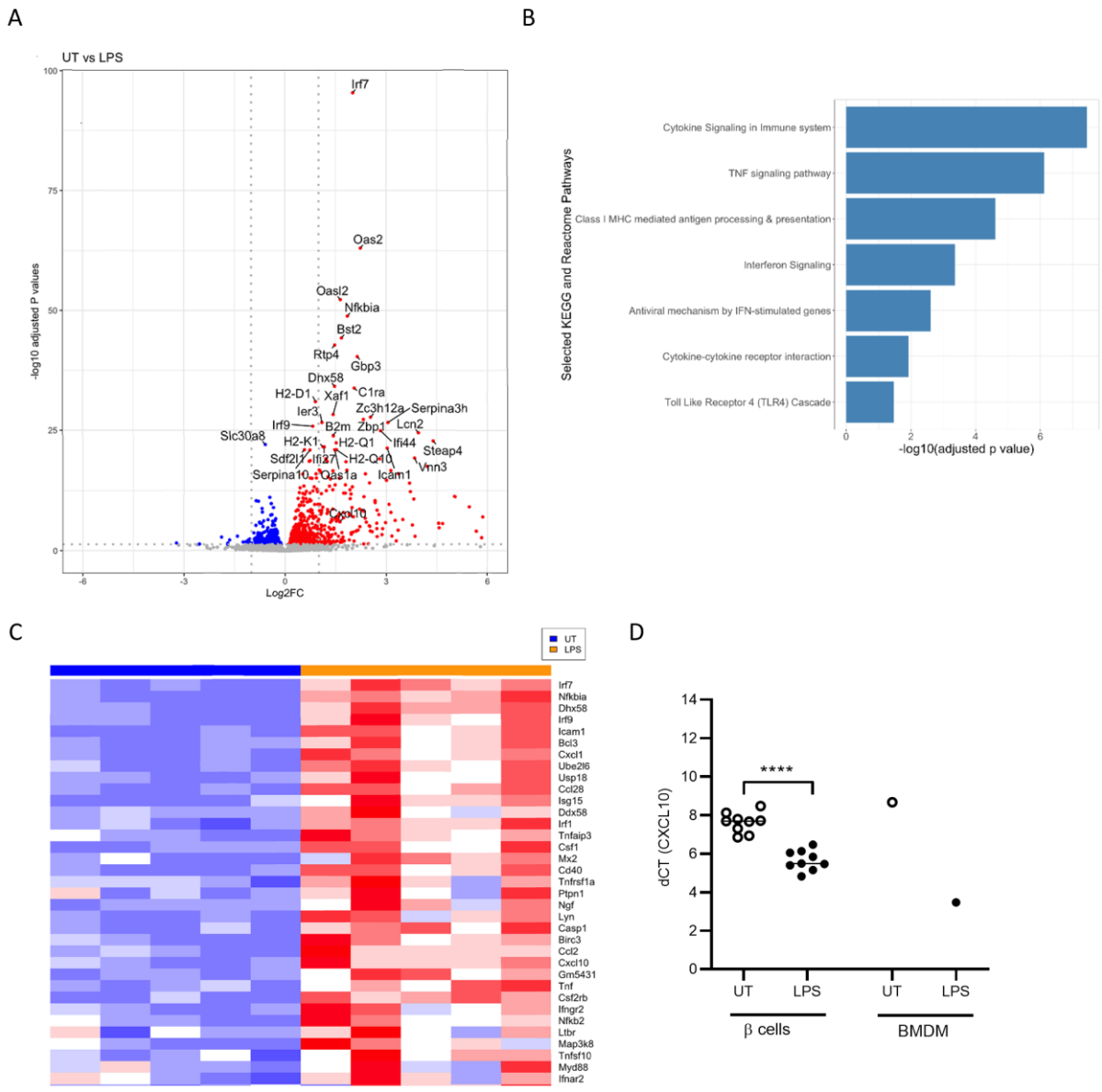


**Figure 7.** Transcriptome analysis of β-cells isolated from whole islets cultured with or without LPS for 48 hours (n=5 independent samples/group). (A) Volcano plot showing genes highly expressed after culturing in media with LPS (red, log2 fold change>0) or without LPS (blue, log2 fold change<0). The top 30 differentially expressed genes (based on adjusted p value) and *Cxcl10* are labeled. (B) Gene ontology pathway analysis of genes upregulated in LPS-treated β-cells compared to control β-cells. The enrichment plot shows selected KEGG and REAC pathways with -log10 adjusted p value. (C) Heatmap of 35 selected genes upregulated in LPS-treated β-cells and have a role in cytokine-signaling pathways as defined by the KEGG and REEAC pathways shown in (B). (D) Real-time PCR expression of *Cxcl10* in untreated and LPS-stimulated β-cells. dCT represents the differential between *Cxcl10* and housekeeping gene (*β-actin*) in amplification cycle values giving threshold positivity (BMDM = bone-marrow derived macrophages). Each data point represents β-cells from an individual Rag-deficient NOD mouse sorted in two independent experiments. Unpaired two-sided Student's t-test, *p****<0,0001*.